Technologies and Processes for the Advancement of Materials

Thermal processing

ISSUE FOCUS ///

VACUUM HEATING / CRYOGENICS

ELECTRICAL HEATING IN VACUUM APPLICATIONS

COMPANY PROFILE ///

TAV Vacuum Furnaces

JANUARY 2021
thermalprocessing.com

CONTENTS ///

COVER PHOTO: BRISKHEAT CORPORATION (2), SHUTTERSTOCK (1) / ILLUSTRATION BY RICK FRENNEA

DEPARTMENTS ///

JANUARY 2021 VOLUME 10 / NUMBER 1

Thermal Processing is published monthly by Media Solutions, Inc., 266D Yeager Parkway Pelham, AL 35124. Phone (205) 380-1573 Fax (205) 380-1580 International subscription rates: $105.00 per year. Postage Paid at Pelham AL and at additional mailing offices. Printed in the USA. POSTMASTER: Send address changes to *Thermal Processing* magazine, P.O. Box 1210 Pelham AL 35124. Return undeliverable Canadian addresses to P.O. Box 503 RPO West Beaver Creek Richmond Hill, ON L4B4R6.

FROM THE EDITOR ///

Setting our sights on 2021

Happy New Year to all our readers in the heat-treat world, and, although New Year's Day wasn't a reset button, it did serve as a turning point into what we all hope will be a brighter future in 2021.

2020 may have been a terrible 48 months (That is how long the year lasted, right?), but *Thermal Processing* didn't let that keep us from our mission of bringing the best heat-treat news and information directly to your mailbox, inbox, and browser.

Despite the pandemic, we've been looking forward to 2021, and you can see some of the results of our quarantine projects in this very issue.

Ceramics has become an integral part of the heat-treating world, and *Thermal Processing* is moving to address this sector of the industry throughout 2021 and beyond. Beginning with our January issue, I'm proud to introduce a brand-new column: Ceramics Works. The experts at CeraMaterials have graciously agreed to take on this duty and bring you this info-packed column that will rotate every other month with our Metal Urgency column.

Please let me know what you think. I'm sure CeraMaterials would love to hear your feedback.

Also, by the time you read this, *Thermal Processing* will have launched what I hope will be a useful and innovative tool to our website. It's our Media page where you'll be able to find out what dozens of heat-treat companies have been posting on their social media, as well as finding a list of helpful blogs, webinars, and podcasts that can direct you to some of the latest insights about thermal processing.

We've been developing this new website feature for months, and we're excited about sharing this with you. If you have a blog, webinar, or podcast you would like to share with the heat-treating community, please let me know about it so it can be included. You'll find easy access to this feature in the Nav Bar on the *Thermal Processing* home page.

Also, to get you primed for the new year, our first issue takes a look at cryogenics and vacuum heating. Our feature articles on these subjects are sure not to disappoint.

In addition to Ceramics Works, make sure you check out what the rest of our columnists have cooked up for January as well. They are always sharing some fascinating information.

And since it is the first of the year, I will take this opportunity to remind all of you that I am always on the lookout for articles and other submissions. It's a great way to share your expertise while shining a spotlight on you and your company at the same time. Hit me up if you have an article idea.

Take stock in the fact that we made it through 2020, so join me and my team as we look to make 2021 even better. It shouldn't be too hard, right?

Happy New Year, and, as always, thanks for reading!

KENNETH CARTER, EDITOR
editor@thermalprocessing.com
(800) 366-2185 x204

CALL FOR ARTICLES Have a technical paper or other work with an educational angle? Let Thermal Processing publish it. Contact the editor, Kenneth Carter, at *editor@thermalprocessing.com* for how you can share your expertise with our readers.

Thermal processing

David C. Cooper
PUBLISHER

EDITORIAL

Kenneth Carter
EDITOR

Jennifer Jacobson
ASSOCIATE EDITOR

Joe Crowe
CONTRIBUTING EDITOR

SALES

Dave Gomez
NATIONAL SALES MANAGER

Ben Keaten
REGIONAL SALES MANAGER

CIRCULATION

Teresa Cooper
MANAGER

Jamie Willett
ASSISTANT

DESIGN

Rick Frennea
CREATIVE DIRECTOR

Michele Hall
GRAPHIC DESIGNER

CONTRIBUTING WRITERS

EDYE S. BUCHANAN
IVO DLOUHÝ
PETER JURČI
MARTIN KUSÝ
JOZEF KRAJČOVIČ
D. SCOTT MACKENZIE
LÝDIA RÍZEKOVÁ-TRNKOVÁ
JASON SCHULZE
JERRY WEINSTEIN
DEL WILLIAMS

Media solutions

PUBLISHED BY MEDIA SOLUTIONS, INC.
P. O. BOX 1987 • PELHAM, AL 35124
(800) 366-2185 • (205) 380-1580 FAX

David C. Cooper
PRESIDENT

Teresa Cooper
OPERATIONS

The furnace configurations either under construction in the company shops or in the early stages of commissioning include rotary hearth, chain conveyor, roller hearth, mesh belt and cast link belt. (Courtesy: Can-Eng Furnaces)

Can-Eng fulfilling contracts for multiple furnaces

Can-Eng Furnaces International LTD has been contracted to deliver a significant number of different furnace types to multiple unique customers in the United States and Canada for the heating and heat treatment of both aluminum and steel closed die forgings. The furnace configurations either under construction in the company shops or in the early stages of commissioning include rotary hearth, chain conveyor, roller hearth, mesh belt and cast link belt. The current uptick in activity from the forging sector represents a major portion of the company's order backlog. These furnaces will be delivered to Georgia, North Carolina, and Ontario and will be used in the production of powertrain, suspension and steering/linkage components for the automotive sector. The demand for new state-of-the-art furnace equipment has been driven by both light weighting initiatives and a shortage of in-house heat treatment capacity. All contracts will be in production by late Q1 2021.

MORE INFO www.can-eng.com

TSX SmartBurner burns up to 100% hydrogen

Tenova, a leading company specialized in innovative solutions for the metals and mining industries, marks a new milestone in the decarbonization of steel production with its TSX SmartBurner for reheating furnaces now ready to be installed in industrial plants with potentially zero carbon dioxide emissions, working in a full range of hydrogen and natural gas mixtures. It is the first flameless burner of a megawatts family that has been tested with 100 percent of hydrogen successfully.

The long tradition of Tenova in flameless leading-edge combustion technology allows it to maintain NOx emissions well below the next future strictest limits — releasing less than 80 mg/Nm^3 @ 5 percent of oxygen with furnace at 1,250°C — also working with 100 percent hydrogen and maintaining an optimal heat-transfer uniformity within the furnace. The quantity of hydrogen can be simply regulated through the burner control logic, allowing steel producers to adapt the fuel mixture to contingent needs without any mechanical intervention.

Tenova's hydrogen flameless combustion system is equipped with the novel smart burner monitoring system (SBMS), which permits it to monitor and optimize the burner's performance, operation, and maintenance thanks to a network of embedded sensors connected to the Tenova digital infrastructure, through secure connection protocols and intrinsic system reliability.

The data collected are post-processed locally on an edge computing unit and remotely on Tenova Cloud, to monitor the status of the burner and implement breakthrough approaches to inspection, maintenance, and tuning, also reducing safety risks related to on-site operations.

"This outstanding achievement paves the way to a significant reduction of the carbon footprint of hot rolling processes without compromising productivity, while leaving steel producers total flexibility to modify the percentage of hydrogen through a simple change in the control software settings. This is not the only reason why we call our burners 'smart.' Thanks to our sensor system technology, we will be able to support our customers remotely to guarantee optimal performances for each burner," said Antonio Catalano, Tenova EVP and head of digital transformation. "Moreover, the SmartBurner Industrial IoT platform represents the cornerstone of the next generation of industrial combustion systems. The most

SEND US YOUR NEWS Companies wishing to submit materials for inclusion in Thermal Processing's Update section should contact the editor, Kenneth Carter, at editor@thermalprocessing.com. Releases accompanied by color images will be given first consideration.

cutting-edge, sustainable technology based on solid experience and extensive know-how: This is what we offer to our customers."

MORE INFO www.tenova.com

Carburizing furnace shipped to captive heat treater

Solar Manufacturing recently shipped a 10-bar gas-quenching vacuum furnace to a captive heat treater in New England. The Model HFL-3836-10IQ-VC features high-pressure gas quenching and vacuum carburizing. The furnace has a graphite insulated hot zone with a work area measuring 24" wide x 24" high x 36" deep and a load weight capacity up to 2,000 pounds. It also has a maximum operating temperature of 2,400°F, temperature uniformity of ±10°F, and is AMS2750F compliant. The furnace is equipped with the state-of-the-art SolarVac® Polaris Control System with carburizing software.

"The research and development done with our sister company, Solar Atmospheres, on the alloy selection, carburizing, and recipe process development was instrumental to the sale of the furnace," said Jason Davidson, Solar's Northeast regional sales manager. "Our customer ultimately decided on Solar Manufacturing due to our dynamic relationship with Solar Atmospheres, which provided an invaluable resource for the end user."

MORE INFO www.solarmfg.com

Solar Manufacturing recently shipped a 10-bar gas-quenching vacuum furnace to a captive heat treater in New England. (Courtesy: Solar Manufacturing)

Grieve now offers jumbo 500°F walk-in batch oven

Grieve No. 1019 is a 500ºF electrically heated walk-in batch oven from Grieve used for curing coatings onto large discs at the customer's facility. Workspace dimensions on this oven measure 18' W x 18' D x 10' H. 260KW are installed in Incoloy-sheathed tubular elements to heat the oven chamber, while a total of 66,000 CFM generated by two 30-HP recirculating blowers provides combination airflow to the workload.

This Grieve walk-in oven features 6-inch insulated walls, aluminized steel exterior and interior and 2-inch thick insulated flooring. (Courtesy: Grieve)

This Grieve walk-in oven features 6-inch insulated walls, aluminized steel exterior and interior, 2-inch thick insulated flooring with built-in oven truck wheel guide tracks and motorized dampers on the intake and exhaust for accelerated cooling of the oven chamber. The oven was sectioned into four pieces for shipping convenience.

All safety equipment required for handling flammable solvents, including explosion-venting door hardware, is provided on No. 1019.

Controls on this jumbo walk-in oven include an SCR power controller.

MORE INFO www.grievecorp.com

FDA allows dry heat for some mask reuse

The FDA announced it will allow the use of dry heat to lower the bioburden on masks used by healthcare workers treating COVID-19 patients.

While not authorizing equipment made by a particular company, guidance released said healthcare providers may use dry heat to reprocess NIOSH-approved filtering facepiece respirators, such as N95s, to enable their reuse by one person. Specifically, the agency recommended that:

» The system can ensure respirator exposure to consistent temperatures of 70°C (158°F) for 60 minutes or 75 °C (167°F) for 30 minutes to guarantee sufficient bioburden reduction while maintaining respirator integrity.

» Chamber temperature can be monitored closely and recorded throughout the cycle to confirm accurate and even distribution of heat.

» The system has highly controlled convective heat transfer (e.g., laboratory oven, industrial convection oven) to avoid the risk of localized over-temperature.

» The system is not a household appliance (e.g., home ovens, pressure cookers, multi-cookers) due to the lack of accuracy and precision in temperature control and the risks of cross-contamination from mixed use.

A study published online in April 2020 in the *Journal of Hospital Infection* showed that dry heat at both 60°C and 70°C for one hour could successfully kill six species of respiratory bacteria and one fungi species, and inactivate the H1N1 indicator virus. After being heated at 70°C for one, two, and three hours, the N95 respirators and surgical face masks showed no changes in their shape and components, the authors noted. The filtering efficiency of bacterial aerosol for N95 respirators was 98 percent, 98 percent and 97 percent after being heated for one, two, and three hours, respectively — greater than the 95 percent efficiency required and similar to the value before being heated (99 percent). The filtering efficiency for surgical face masks was 97 percent, 97 percent, and 96 percent for one, two and three hours of heating, respectively, all of which were also similar to the value before being heated (97 percent), the study found.

The use of dry heat to reduce bioburden is only intended to supplement existing single-user reuse recommendations from the Centers for Disease Control and Prevention (CDC), such as storing a used N95 mask in a breathable paper bag for a minimum of five days between each use, according to the FDA.

Bioburden reduction systems can play an important role in the ongoing efforts to help address shortages of filtering facepiece respirators, said Dr. Binita Ashar, director of the Division of Surgical Devices in FDA's Center for Devices and Radiological Health.

"There exists sufficient evidence demonstrating that there is a reduction of microbial load on certain respirators when exposed to certain dry heat parameters," Ashar said in a news release.

MORE INFO www.medicaldesignandoutsourcing.com

Tenova EAF will be supplied to Valbruna in Canada

Tenova, a leading company specialized in innovative solutions for the metals and mining industries, was awarded a contract by Valbruna ASW Inc., for the supply of a

Tenova was awarded a contract by Valbruna ASW Inc., for the supply of a new EAF (electric arc furnace). (Courtesy: Tenova)

new EAF (Electric Arc Furnace). Valbruna ASW Inc. is a premier specialty steel-maker and the EAF will be installed at its facility located in Welland, Ontario (Canada).

The scope of the supply includes the latest generation of the EAF unit, which will replace the existing one. Tenova will also provide the associated auxiliary equipment, the material handling system, including bins, batteries, hoppers, and conveyor belts, for the charging of the ladle and of the EAF and the complete automation system. The complete management of this plant will be fully automatized and integrated in the new the EAF process control system.

The new EAF will guarantee an increase in the plant's hourly melt shop production rate and the effectiveness and reliability in the production of high-quality steel and stainless steel.

The new automation system brings several advantages, which will enhance the level of efficiency of the plant. In particular, it guarantees the correct and effective execution of the working cycle in relation to the production of different steel grades. It also optimizes the working parameters and the storage of production data. In addition, the safety of the operators in the plant is significantly improved and the system complies with the most stringent safety standards.

The new EAF will be equipped with Tenova's state-of-the-art electronic regulation TDRH 4.0 (Tenova Digital Electronic Regulation) system. TDRH 4.0 can provide a significant reduction in the electrical consumption of the EAF itself and ensures excellent arc stability. This updated version has additional features mainly dedicated to self-diagnostic, faults identification and compensation, as well as auto-calibration (self-learning) and adjustment of the regulation parameters. These functions aim to preserve the optimized electrodes regulation performances over the time.

"Our long-lasting relationship with the Valbruna Group is witnessed by several projects in its plants in Italy (Vicenza and Bolzano), where we implemented some of our technologies to increase safety, sustainability and production," said Marco Longobardo, digital products manager in Tenova. "This is also the aim of this new project in Canada, where the plant will be a technological reference in North America for the production of stainless steel."

MORE INFO www.tenova.com

PCI announces 2021 directors, executive officers

The Powder Coating Institute (PCI) announced its 2021 board of directors and executive officers. They are:

» President: John Cole, president, Parker Ionics.

» Vice president: Chris Merritt, general manager, Gema USA, Inc.

» Secretary/treasurer: Shelley Verdun, business manager, Powder Coatings, PPG.

» Past president: Suresh Patel, sales director — director, North America business development, BASF/Chemetall US Inc.

In addition, serving on the board of directors for 2021 are:

» Greg Dawson, zone manager, Nordson Corporation,

» Rick Gehman, president, Keystone Koating LLC.

» Marty Korecky, business specialist — business systems, AkzoNobel Powder Coatings.

» John Sudges, sales manager, Midwest Finishing Systems Inc.

» Tom Whalen, vice president sales & marketing, TCI Powder Coatings.

» Paul West, director of marketing, Sun Polymers International, Inc.

» Mike Withers, architectural segment leader, Axalta Coating Systems.

PCI congratulated long-time member and recent PCI executive officer Sue Ivancic on her recent retirement from Nordson Corporation after 42 years with the company. Ivancic joined the PCI Board of Directors in 2017 after serving as PCI's education committee chair for several years. She brought decades of experience in the powder coating industry along with a fresh perspective to the board and moved into the officer rotation in 2019. Ivancic dedicated countless hours to PCI business, including her involvement when Nordson hosted the PCI workshops.

Formed in 1981 as a non-profit organization, the Powder Coating Institute (PCI) represents the powder coating industry, promotes powder coating technology, and communicates the benefits of powder coating to manufacturers, consumers, and government. PCI works to advance the use of powder coating as an economical, non-polluting, and high-quality finish for industrial and consumer products.

MORE INFO www.powdercoating.org

From left, Mike Johnson, director of sales; Wes Hoffman, FSO; and Bob Hill, president. (Courtesy: Solar Atmospheres)

Northrop Grumman recognizes Solar Atmospheres

Northrop Grumman Defense Systems recognized Solar Atmospheres of Western PA (SAWPA) as a top-performing supplier in 2020 with the Outstanding Customer Service Award. As a global leader of military and DoD critical hardware, Northrop Grumman Defense Systems offers security to customers across the globe through the operational excellence SAWPA provides to customers. Solar Atmospheres appreciates the recognition and looks forward to supporting the future needs of this partnership with a mutual goal to keep all Americans safe.

MORE INFO www.solaratm.com

SCA adds more large furnace capacity to inventory

Solar Atmospheres of California (SCA) recently added additional large furnace capacity to their already extensive inventory of vacuum equipment. The furnace was specifically designed to process a variety of materials that require optimum performance during controlled heating, controlled cooling, vacuum processing, positive pressure processing, and differential pressure processing. SCA works very closely with sister company Solar Manufacturing to design and fabricate equipment to provide repeatable mistake-proof processing while meeting all prime requirements and AMS 2750.

Key equipment performance characteristics include:

» 84-inch diameter x 144-inch long robust and energy efficient all graphite and CFC hot zone.

» Temperature uniformity ±10°F.

» Dual 35-inch diffusion pumping systems capable mid 10-6 Torr range.

» Maximum operating temperature of 2,650°F.

» Maximum loading of 50,000 pounds.

» 2-Bar high performance 800 HP cooling system (argon, nitrogen and helium).

» SolarVac Polaris® electrical control system.

"We are very pleased to add the additional large furnace capacity. Each new furnace installation is built on a building block approach from the personal knowledge and experience accumulated by operating previous furnace models," said SCA President Derek Dennis. "I really appreciate the ability to bounce different 'out of the box' ideas to our manufacturing team, who then takes those ideas and makes them a reality. Often, the team takes the ideas to another level before the final build plans go to the shop floor. It is this valuable collaboration between companies that allows Solar to lead the industry in material processing and furnace manufacturing. The new furnace will bolster SCA's position as a leader in the heat-treat industry on the West Coast, and provide our valuable customers with the very best quality, on-time delivery and repeatable value-added service, coupled with the best customer service in the industry."

MORE INFO www.solaratm.com

SVT provides DoD with vacuum oil quenching furnace

A division of the U.S. Department of Defense uses a vacuum furnace with low-pressure carburizing from Seco/Warwick Group to bolster its capability to ensure supply chain reliability.

A unique vacuum heat-treating furnace from Seco/Vacuum (SVT), a Seco/Warwick Group company, with integral oil quench will also be equipped with high-pressure gas quench as well as low-pressure carburizing

As a critical supplier of aerospace components to the U.S. Department of Defense, this new vacuum oil quenching furnace will be able to handle any of the functions of the department's existing heat-treatment furnaces. (Courtesy: Seco/Vacuum)

capabilities, a "Swiss Army Knife" version of a heat-treating furnace.

As a critical supplier of aerospace components to the U.S. Department of Defense, this new vacuum oil quenching furnace will be able to handle any of the functions of the department's existing heat-treatment furnaces, either in a redundant role or to provide additional capacity. Also, the addition of low-pressure carburizing (LPC) and high-pressure gas quenching (HPGQ) is new to this location. Aerospace-related process applications conducted at this facility, for which the new furnace will be equipped, include steel hardening, surface engineering, vacuum annealing, nickel alloy processing, and titanium heat treatment.

"Assuring redundancy in heating needs of this location was critical," said Piotr Zawistowski, managing director of Seco/Vacuum. "Seco/Vacuum has demonstrated competence and experience in delivering customized solutions. As well, vacuum oil quenching was a critical process need and LPC, combined with HPGQ, allows materials engineers with new options."

The order is the result of two years of effort. While this is not SVT's first order for DOD, it is one of the most advanced engineering projects to date.

Defense customer specializes in the repair and maintenance of aerospace components. The furnace not only performs vacuum oil quenching, but it also offers the ability to gas quench at 15 bar with nitrogen and 6 bar with argon and heat with diffusion pump vacuum levels.

"Any commercial or in-house heat-treat shop looking for a partner to design and deliver an advanced and unique custom solution could gain significant benefit by collaborating with us," said Maciej Korecki, VP, vacuum business segment at Seco/Warwick. "We not only provide six unique, time-tested vacuum furnace technologies in use around the globe, we are very comfortable with our ability to innovate to solve special applications."

MORE INFO www.secowarwick.com

Babcock orders PEMA shipbuilding automation lines

Babcock International Group, the aerospace and defense company, has placed an order for an extensive set of PEMA welding and production lines for shipbuilding at its Rosyth site in Scotland. In total, the order includes three lines — PEMA Thin plate panel line, PEMA Micro panel line, and PEMA T-beam fabrication line.

Each PEMA production line is based on modern shipbuilding technology that enables Babcock to raise its level of automation. PEMA Thin plate panel line is equipped with the latest technologies, such as plate edge milling and robotic welding, which enable high-quality production of various panel types. PEMA T-beam fabrication line is designed to make straight T-beams without any additional straightening processes.

PEMA Micro panel line consists of a customized solution that first assembles the profiles before they are welded with a compact Vision robotics solution. The main benefit of the line is that it automatizes micro panel production, but also other small- to medium-sized constructions. The control of the robotic system is based on PEMA WeldControl 200 software, which enables easy weld path creation and robot programming.

The advanced shipbuilding automation lines are customized according to Babcock's production needs to efficiently weld deck panels and bulkheads. For Babcock, the lines bring increased capability in welding and handling, the improved manufacturing quality of ship structures, and streamlined production processes while requiring less manual work. The lines will initially be used for the Type 31 general purpose frigate program being built and assembled at its Rosyth facility.

Pemamek's turn-key delivery also includes installation and commissioning, testing, training, production support, and recommended spare parts. A comprehensive preventive maintenance agreement package is also included in the scope of supply.

Pemamek Ltd, founded in 1970, is a global welding and production automation leader. With the extensive 50-year experience in welding and production automation, Pemamek is dedicated to helping heavy fabrication industries, such as shipbuilding, wind energy, and power generation industry, to raise the level of productivity.

MORE INFO www.pemamek.com

INDUSTRIAL HEATING EQUIPMENT ASSOCIATION

IHEA educates the industry in person, online

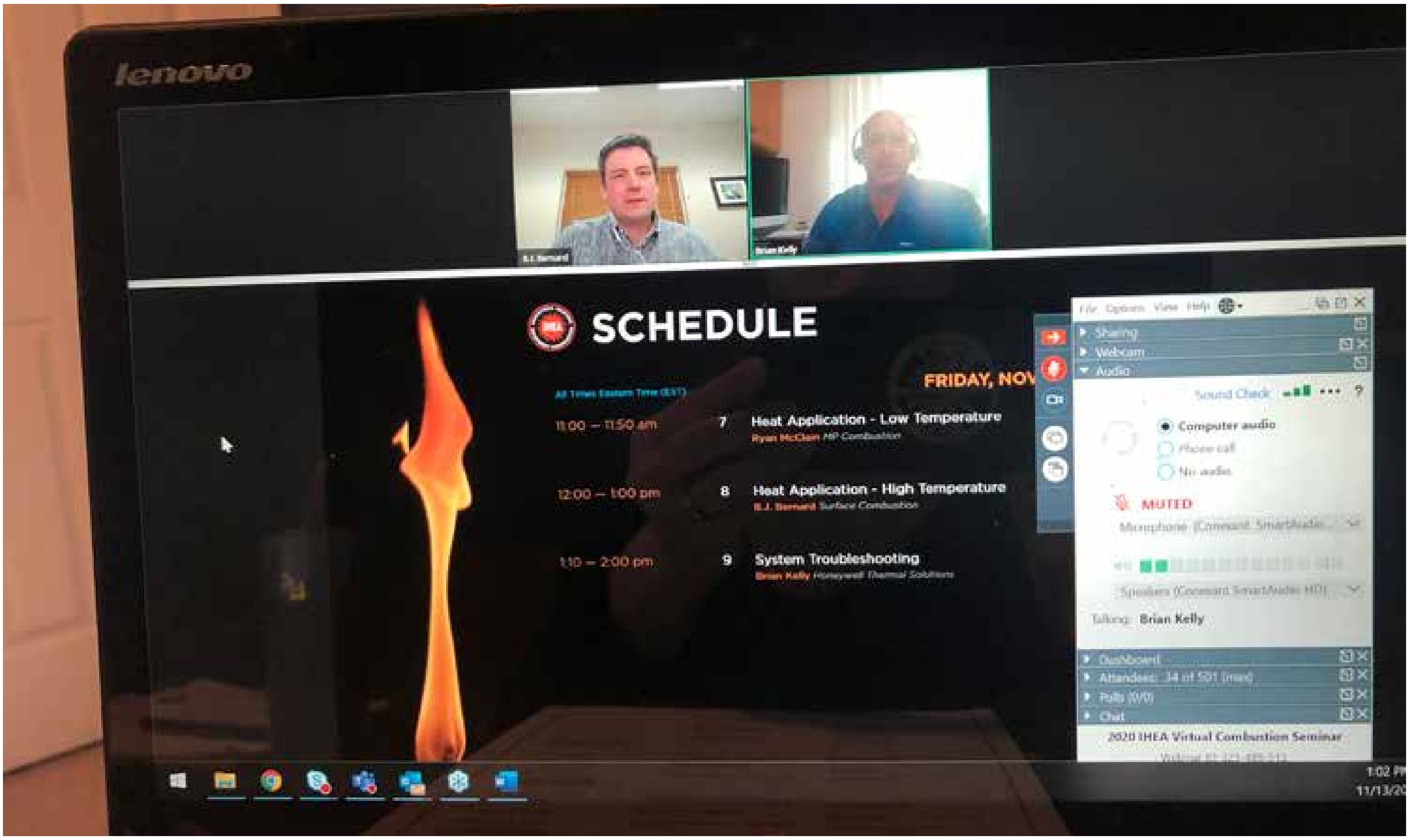

Looking ahead … Register now!
Fundamentals of Industrial Process Heating
Winter Online Course
January 25–March 7, 2021

IHEA's Fundamentals of Industrial Process Heating Online Learning Course has been a successful source of high-level learning to those in the industrial heat processing industry for more than 10 years. Registration for the 2021 winter course is now open and, for the past few years, the course has sold out, so early registration is encouraged. Scheduled to begin January 25, the six-week class will run through March 7. The flexible online format and interactive forums with other students, along with scheduled office hours with the instructor, are just a few of the benefits of this program.

The course is ideal for students to learn in a virtual format while at home or in the office. It is affordable and allows students to go at their own pace. The course offers indispensable tools to industrial process heating operators and users of all types of industrial heating equipment. Throughout the in-depth online course, students learn safe, efficient operation of industrial heating equipment, how to reduce energy consumption, and ways to improve the bottom-line. The course content provides an excellent overview of the essential areas used throughout the industry.

The curriculum includes the basics of heat transfer, fuels and combustion, energy use, furnace design, refractories, automatic control, and atmospheres as applied to industrial process heating. Weekly coursework, quizzes, and a final exam project are administered to guide students on their progress and evaluate their knowledge of the material. For a complete listing of the topics covered, visit www.ihea.org/event/FundamentalsWinter21.

This online course is a terrific value for IHEA members and nonmembers alike, considering no travel expenses are involved and there is no time out of the office.

A former online student said, "Because of balancing an extremely busy workload and family life, I am not able to be on a regular schedule or take time in the evening to travel to a class. The advantage for me is that I can check in when time permits and still stay current on all activities. The course information is directly related to my work, and I found it to be very beneficial."

Registration for the Fundamentals course is open now through January 18, 2021, at www.ihea.org/event/FundamentalsWinter21. Cost for IHEA members is $750 or one member voucher, and cost for non-members is $925, which includes an electronic course handbook, course instruction, quizzes and projects, class forums, and the opportunity to contact the instructor throughout the course. Printed materials are available for an additional fee.

Due to the coronavirus pandemic, the Industrial Heating Equipment Association (IHEA) offered its Fall Seminars through a virtual platform in 2020.

SUCCESSFUL VIRTUAL SEMINARS

This year, the Industrial Heating Equipment Association (IHEA) offered its Fall Seminars through a virtual platform. With the assistance of speakers from member companies, they conducted the Combustion Seminar and Safety Standards and Codes Seminar for three days each in mid-November. The seminar agendas were pared down to offer sessions that would fit best in a virtual training format. Speakers revised their presentations and adapted to the virtual program almost seamlessly. IHEA offered each seminar over a three-day period during consecutive weeks to allow attendees the option to register for both seminars, and it was a great success.

Both seminars had more than 30 attendees, and speakers were available online to field questions after the presentations. The overall feedback for the seminars was terrific. Although everyone agrees we would rather hold in-person events, the comments reflect great appreciation for the virtual training. IHEA is happy to continue to provide educational support to the industry, no matter how it's delivered.

INFRARED HEATS UP ALABAMA

The Infrared Equipment Division of IHEA (IRED) partnered with the Chemical Coaters Association International for a successful (and safe) event at the Alabama Power Company in October. Masked up and socially distant, attendees spent a day and a half with industry experts learning everything from pretreatment and powder materials to curing processes and testing equipment for powder coating. Attendees enjoyed the live demonstrations and time in the lab, powder coating and curing a part up close and personal. Instructors were on hand throughout the seminar to guide attendees and answer questions. It was great to have in-person training again.

The Infrared Equipment Division of IHEA (IRED) partnered with the Chemical Coaters Association International for a successful (and safe) event at the Alabama Power Company in October.

Overall ratings for the seminar were excellent.

Attendee comments included:

» "All speakers were very knowledgeable. Covered a wide variety of topics and made very good connections — that was one of the most helpful parts of the seminar."

» "Great range of topics. Speakers were very personable and informative."

» "Very detailed speakers, very useful information for all levels. I will be returning to the next one with more members of our team."

IHEA 2021 CALENDAR OF EVENTS

JANUARY 25–MARCH 7

Fundamentals of Industrial Process Heating

6-week online course beginning January 25, 2021

This course is designed to give the student a fundamental understanding of the mechanisms of heat transfer within an industrial furnace and the associated losses and the operation of a heating source either as fuel combustion or electricity. All concepts are derived mathematically with limited use of "rules of thumb."

For details on IHEA events, go to www.ihea.org/events

INDUSTRIAL HEATING EQUIPMENT ASSOCIATION

P.O. Box 679 I Independence, KY 41051

859-356-1575 I www.ihea.org

JERRY WEINSTEIN, PH.D.
MATERIALS SCIENCE ENGINEER /// CERAMATERIALS

Ceramics cover a variety of chemistries and applications where temperature, strength, precision, and thermal resistance are key.

Tailoring advanced ceramics to meet niche properties

Ceramics are traditionally described as inorganic, nonmetallic solids that are prepared from powdered raw materials and fabricated into products through the application of heat. Advanced ceramics represent an "advancement" over this traditional definition, with compositions ranging over oxides, nitrides, silicides, carbides, and combinations thereof. Key characteristic properties of advanced ceramics are hardness, strength, low electrical conductivity, and brittleness, although all properties can be tailored to meet specific niche properties through composition and processing. New materials or new combinations of existing materials have been designed that exhibit surprising variations on the properties traditionally ascribed to ceramics. As a result, there are now ceramic products that are as tough and electrically conductive as some metals. Ceramics cover a wide array of chemistries and applications where temperature, strength, precision, and thermal resistance are key to operational success and safety.

Advanced ceramic materials are used throughout thermal processing for many applications. The major types of advanced ceramics used in thermal processing will be reviewed by general chemistry and touch upon some of the applications within thermal processing.

Aluminas (aluminum oxide, Al_2O_3) are the most commonly used technical ceramics due to their generally useful properties and good price/performance ratio and are suitable for most industry applications (See Table 1). Alumina, or aluminum oxide, is a hard, dense material with good strength and corrosion and erosion resistance, along with high electrical volume resistivity as well as low loss characteristics at high frequencies. The higher purity results in higher mechanical properties but higher costs. Alumina sees application from aerospace to medical, from bearings to analytical instrumentation, from electrical standoffs to semiconductor processing. In addition, these materials lend themselves well to be hermetically sealed to metals through metallizing and brazing methods, often used in the electrical feedthrough for vacuum and controlled atmosphere furnaces.

Standard shapes include plates, rods, tubes, and vessels. Alumina is used for many applications including kiln furniture and fixturing, wear-resistant plates, feedthrough tubes, support rods, and grinding media. Alumina crucibles are also used in the melting of high-temperature alloys as crucibles and pouring cups, although more limited due to poor thermal shock capability of alumina.

Zirconia (ZrO_2) is a very hard and durable material with low thermal conductivity, electrical conductivity, and high strength (See Table 2). With certain densification additives, the material has a higher resistance to corrosion and melting point than alumina. Zirconia is used in oxygen sensors, feedthrough tubes, kiln furniture, grinding media, dental teeth, as well as other technical applications.

These are several of the most popular grades of zirconia:

» Magnesia Partially Stabilized Zirconia (MgO-ZrO_2) is mostly used for higher temperature applications, as it is stabilized against phase transformations at elevated temperatures. Often used for furnace and hot high-pressure fixturing.

Al_2O_3 Properties	Units	Test	85%	90%	94%	96%	98.5%	99.5%	99.8%	99.9%
Color			White	White	White	White	White	Ivory	Ivory	Ivory
Density	g/cm^3	ASTM-C20	3.42	3.60	3.70	3.72	3.80	3.90	3.92	3.92
Avg Crystal Size	MICRONS	ASTM-E112	6	4	8	6	6	6	6	3
Flexural Strength (MOR)	MPa (psi x 10^3) @ 68°F | 20°C	ASTM-F417	296 (43)	338 (49)	352 (51)	358 (52)	375 (54)	379 (55)	390 (57)	400 (58)
Elastic Modulus	GPa (psi x 10^6) @ 68°F | 20°C	ASTM-C848	221 (32)	276 (40)	303 (44)	303 (44)	350 (51)	370 (54)	380 (55)	386 (56)
Poisson's Ratio	@ 68°F | 20°C	ASTM-C848	0.22	0.22	0.21	0.21	0.22	0.22	0.22	0.22
Compressive Strength	MPa (psi x 10^3) @ 68°F | 20°C	ASTM-C773	1930 (280)	2482 (360)	2103 (305)	2068 (300)	2500 (363)	2600 (377)	2650 (384)	2700 (392)
Hardness	R45N GPa (kg/mm^2)	ROCKWELL 45N KNOOP 1000 gm	73 9.4 (960)	75 10.4 (1058)	78 11.5 (1175)	78 11.5 (1175)	82 13.7 (1400)	83 14.1 (1440)	83 14.1 (1440)	86 14.5 (1480)
Tensile Strength	MPa (psi x 10^3) @ 77°F | 25°C	ACMA TEST #4	155 (22)	221 (32)	193 (28)	221 (32)	248 (36)	262 (38)	272 (39)	283 (41)
Fracture Toughness	MPa m$^{1/2}$ K_{Ic}	NOTCHED BEAM	3 - 4	3 - 4	4 - 5	4 - 5	4 - 5	4 - 5	4 - 5	4 - 5
Thermal Conductivity	W/m K @ 68°F | 20°C	ASTM-C408	16.0	16.7	22.4	24.7	27.5	30.0	31.0	33.0
Coefficient of Thermal Expansion	1 x 10^{-6}/°C @ 25 - 1000°C	ASTM-C372	7.2	8.1	8.2	8.2	8.2	8.2	8.2	8.2
Specific Heat	J/kg*K @ 212°F | 100°C	ASTM-E1269	920	920	880	880	880	880	880	870
Thermal Shock Resistance	Δ Tc °C	WATER QUENCH	300	250	250	250	200	200	200	200
Dielectric Strength @ 6.35mm	ac-kV/mm ac V/mil	ASTM-D116	9.4 240	8.3 210	8.3 210	8.3 210	8.7 220	8.7 220	8.7 220	8.7 220
Dielectric Constant	1 MHz @ 77°F | 25°C	ASTM-D150	8.2	8.8	9.1	9.0	9.6	9.7	9.8	9.8
Dielectric Loss (Tan Delta)	1 MHz @ 77°F | 25°C	ASTM-D150	0.0009	0.0004	0.0004	0.0002	0.0002	0.0001	< 0.0001	< 0.0001
Volume Resistivity @ 77°F | 25°C @ 932°F | 500°C @ 1832°F | 1000°C	ohm-cm	ASTM-D1829	> 10^{14} 4 x 10^8 -	> 10^{14} 4 x 10^8 5 x 10^5	> 10^{14} 4 x 10^9 5 x 10^5	> 10^{14} 4 x 10^9 1 x 10^6	> 10^{14} 2 x 10^{10} 2 x 10^6	> 10^{14} 2 x 10^{10} 2 x 10^6	> 10^{14} 2 x 10^{11} 2 x 10^7	> 10^{15} 1 x 10^{12} 1 x 10^7

Table 1: Alumina properties. (Charts courtesy: CeraMaterials)

» Yttria Partially Stabilized Zirconia (Y-ZrO_2) is a much fine-grained microstructure predominantly "transformation toughened" tetragonal phase resulting in relatively high strength and toughness (crack resistance), along with good corrosion and wear resistance when used at temperatures below 500°C. The hipped (high isostatic press) material has better mechanical properties and higher cost.

» Alumina Toughened Zirconia (ZTA) provides about 25 percent greater strength than alumina at a lower cost than stabilized zirconias, with higher toughness, hardness, and wear resistance than alumina. It is good for high temperature applications.

Ceramic nozzles, commonly used in the casting of molten steel in continuous casters. (Courtesy: CeraMaterials)

Properties	Units	Test	Zirconia Toughened Alumina	Magnesia Partially Stablized Zirconia	Yttria Partially Stablized Zirconia Sintered	Yttria Partially Stablized Zirconia HIPped
Color			White	Ivory	Ivory	Gray
Density	g/cm^3	ASTM-C20	4.01	5.72	6.02	6.07
Avg Crystal Size	MICRONS	ASTM-E112	2	25	1	1
Flexural Strength (MOR)	MPa (psi x 10^3) @ 68°F | 20°C	ASTM-F417	450 (65)	900 (131)	1240 (180)	1720 (249)
Elastic Modulus	GPa (psi x 10^6) @ 68°F | 20°C	ASTM-C848	360 (52)	200 (29)	210 (30)	210 (30)
Poisson's Ratio	@ 68°F | 20°C	ASTM-C848	0.30	0.30	0.30	0.30
Compressive Strength	MPa (psi x 10^3) @ 68°F | 20°C	ASTM-C773	2900 (421)	1750 (254)	2500 (363)	2500 (363)
Hardness	R45N Gpa (kg/mm^2)	ROCKWELL 45N KNOOP 1000 gm	85 14.5 (1475)	77 11.8 (1200)	81 12.7 (1300)	81 12.7 (1300)
Tensile Strength	Mpa (psi x 10^3) @ 77°F | 25°C	ACMA TEST #4	290 (42)	483 (70)	-	-
Fracture Toughness	MPa m$^{1/2}$ K_{Ic}	NOTCHED BEAM	5 - 6	11	13	13
Thermal Conductivity	W/m K @ 68°F | 20°C	ASTM-C408	27.0	2.2	2.2	2.2
Coefficient of Thermal Expansion	1 x 10^{-6}/°C @ 25 - 1000°C	ASTM-C372	8.3	10.2	10.3	10.3
Specific Heat	J/kg*K @ 212°F | 100°C	ASTM-E1269	885	400	400	400
Thermal Shock Resistance	Δ Tc °C	WATER QUENCH	300	350	350	350
Dielectric Strength @ 6.35mm	ac-kV/mm ac V/mil	ASTM-D116	9.0 228	9.4 240	9.0 228	9.0 228
Dielectric Constant	1 MHz @ 77°F | 25°C	ASTM-D150	10.6	28.0	29.0	29.0
Dielectric Loss (Tan Delta)	1 MHz @ 77°F | 25°C	ASTM-D150	0.0005	0.001	0.001	0.001
Volume Resistivity @ 77°F | 25°C @ 932°F | 500°C @ 1832°F | 1000°C	ohm-cm	ASTM-D1829	> 10^{14} 2 x 10^9 3 x 10^6	> 10^{13} 2 x 10^4 < 10^3	> 10^{13} 2 x 10^4 < 10^3	> 10^{13} 2 x 10^4 < 10^3

Table 2: Zirconia properties.

Silicon carbide materials (SiC) have very high hardness and rigidity with low density and some electrical conductivity, valuable in applications that require a combination of light weight and mechanical strength, even at high temperatures (See Table 3). Silicon carbide is used as a support and shelving material in high-temperature air kilns as well as used for heating elements for firing ceramics, glass fusing, or glass casting. SiC also makes the best body armor, as well as having wide use in semiconductor processing. SiC also has excellent erosion resistance and is used to line slurry handling equipment and mechanical seals.

There are several types of silicon carbide used in thermal processing. The more popular ones include:

Nitride bonded silicon carbide is formed near net shape with a hard, thick surface skin that is strong, has excellent thermal shock characteristics and wear resistance. Thermal processing applications include:

» Kiln furniture, pusher plates, and muffle liners.

» Liners for cyclone and hydrocyclone applications.

» Liners for pipe, immersion heater tubes, "pig" tube liners, and spool linings.

» Vortex finders, spray nozzles, thimbles, and dip tubes.

» Dust collector components.

Reaction Bonded Silicon Carbide has some residual silicon metal which limits its temperature of use, but it has excellent wear, impact, and chemical resistance. The strength of RBSC is almost 50 percent greater than that of most nitride bonded silicon carbides and can be densified near net shape into a variety of shapes, including cone and sleeve shapes, as well as more complex engineered pieces designed for equipment involved in the handling and processing of raw materials. Applications of this SiC include:

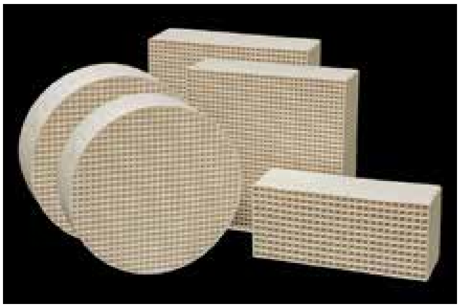

Cordierite Honeycomb, commonly used as molten metal casting filters and air filter substrates for automotive catalytic converters. (Courtesy: CeraMaterials)

» Micronizers (for powder processing).

» Liners for cyclone and hydrocyclones.

» Boiler tube ferrules.

» Kiln furniture, pusher plates, muffle liners, plates, saggers, and setters.

» Spray and sand blast nozzles.

Recrystallized Silicon Carbide has been designed for a multitude of low mass kiln furniture applications including:

» Plates, saggers, boats, setters, muffle liners, kiln furniture.

» Burner nozzles, pilot, and flare tops.

» Structural furnace components.

Sintered Silicon Carbide is distinguished by exceptionally high strength that stays nearly constant up to very high temperatures (approximately 1,600°C) with no degradation over time. The material displays an extremely high corrosion resistance in acidic and basic media and is maintained up to very high temperatures. Properties are outstanding among high-temperature ceramics, complemented by high thermal shock resistance, high thermal conductivity, high resistance to wear, and hardness close to that of a diamond. Ideal for extremely demanding applications including:

» Mechanical seals, bearing bushes, and valve seats and components.

» High-temperature burner nozzles.

» Kiln furniture for very high application temperatures.

» High end liners for cyclones, hydrocyclones, and slurry pumps.

» Note that other carbides commercially available include:

» Boron Carbide (B_4C), which is used as sand blast nozzles and body armor.

» Tungsten carbide (WC), which sees applications in cutting and grinding tooling and fixturing.

Silicon nitrides (Si_3N_4) are distinguished by their high-temperature strength, demonstrating an exceptional combination of mechanical and thermal properties (See Table 4). One particular advantage of silicon nitride is its high strength-to-weight ratio, which compares favorably even with metallic nickel-based "superalloys." Silicon nitrides are used in severe-service environments requiring a combination of extreme flexural strength and toughness. Applications include:

» Gas injection, riser tubes, and immersion heaters in metal casting.

» Thermocouple protection tubes.

» Liners for valves, mechanical seals, and components.

» Grinding media and roller bearings.

Cordierite ($2MgO{\cdot}2Al_2O_3{\cdot}5SiO_2$) ceramics have low thermal expansion, providing excellent thermal shock resistance, but a more limited temperature of use range (~1,200°C max) (See Table 5).

» Plates, saggers, boats, setters, and kiln furniture in air furnaces.

» Heating element holders and insulators.

» Hot gas filters, candle filters, and recuperators.

Properties	Units	Test	Reaction Bonded Silicon Carbide	Direct Sintered Silicon Carbide	CVD Sintered Silicon Carbide	Reaction Bonded Boron Carbide	Hot Pressed Boron Carbide	Tungsten Carbide
Color			Black	Black	Black	-	Black	Gray
Density	g/cm^3	ASTM-C20	3.10	3.15	3.21	2.65	2.5	14.90
Avg Crystal Size	MICRONS	ASTM-E112	12	4	-	-	15	1
Flexural Strength (MOR)	MPa (psi x 10^3) @ 68°F | 20°C	ASTM-F417	462 (67)	480 (70)	470 - 520 (68 - 75)	250 (36)	410 (59)	2330 (338)
Elastic Modulus	GPa (psi x 10^6) @ 68°F | 20°C	ASTM-C848	393 (57)	410 (59)	435 - 460 (63 - 67)	379 (55)	460 (67)	614 (89)
Poisson's Ratio	@ 68°F | 20°C	ASTM-C848	0.20	0.21	0.21	0.18	0.17	-
Compressive Strength	MPa (psi x 10^3) @ 68°F | 20°C	ASTM-C773	2700 (392)	3500 (508)	-	1721 (250)	-	4343 (630)
Hardness	R45N GPa (kg/mm^2)	ROCKWELL 45N KNOOP 1000 gm	- 24.5 (2500)	- 27.4 (2800)	- 27 (2750)	- 25.5 (2600)	27 (2750)	15.2 (1548)
Tensile Strength	MPa (psi x 10^3) @ 77°F | 25°C	ACMA TEST #4	307 (44.5)	-	-	-	-	-
Fracture Toughness	MPa m$^{1/2}$ K_{Ic}	NOTCHED BEAM	4	4	3.5	3 - 4	2.5	24
Thermal Conductivity	W/m K @ 68°F | 20°C	ASTM-C408	125.0	150.0	140.0	50.0	90.0	84.0
Coefficient of Thermal Expansion	1 x 10^{-6}/°C @ 25 - 1000°C	ASTM-C372	4.3	4.4	4.6	4.5	5.6	5.9
Specific Heat	J/kg*K @ 212°F | 100°C	ASTM-E1269	800	800	665	-	-	-
Thermal Shock Resistance	Δ Tc °C	WATER QUENCH	400	300	-	-	-	-
Dielectric Strength @ 6.35mm	ac-kV/mm ac V/mil	ASTM-D116	-	-	-	-	-	-
Dielectric Constant	1 MHz @ 77°F | 25°C	ASTM-D150	-	-	-	-	-	-
Dielectric Loss (Tan Delta)	1 MHz @ 77°F | 25°C	ASTM-D150	-	-	-	-	-	-
Volume Resistivity @ 77°F | 25°C @ 932°F | 500°C @ 1832°F | 1000°C	ohm-cm	ASTM-D1829	< 10^3 < 10^3 < 10^3	~ 10^5 ~ 10^3 ~ 10^2	< 0.10 - > 10^5 - -	< 10^3 < 10^3 < 10^3	< 10^2 - -	< 10^3 < 10^3 < 10^3

Table 3: Silicon Carbide, Boron Carbide, and Tungsten Carbide properties.

Properties	Units	Test	Silicon Nitride (Glass HIPped)	High Temp Silicon Nitride (Glass HIPped)
Color			Gray	Gray
Density	g/cm^3	ASTM-C20	3.21	3.22
Avg Crystal Size	MICRONS	ASTM-E112	-	-
Flexural Strength (MOR)	MPa (psi x 10^3) @ 68°F | 20°C	ASTM-F417	1000 (145)	900 (131)
Elastic Modulus	GPa (psi x 10^6) @ 68°F | 20°C	ASTM-C848	310 (45)	310 (45)
Poisson's Ratio	@ 68°F | 20°C	ASTM-C848	0.27	0.27
Compressive Strength	MPa (psi x 10^3) @ 68°F | 20°C	ASTM-C773	2500 (363)	-
Hardness	R45N Gpa (kg/mm^2)	ROCKWELL 45N KNOOP 1000 gm	- 16 (1630)	- 16 (1630)
Tensile Strength	Mpa (psi x 10^3) @ 77°F | 25°C	ACMA TEST #4	-	630 (91)
Fracture Toughness	MPa m$^{1/2}$ K_{Ic}	NOTCHED BEAM	6.5	6.0
Thermal Conductivity	W/m K @ 68°F | 20°C	ASTM-C408	34	38
Coefficient of Thermal Expansion	1 x 10^{-6}/°C @ 25 - 1000°C	ASTM-C372	3.7	3.1
Specific Heat	J/kg*K @ 212°F | 100°C	ASTM-E1269	-	724
Thermal Shock Resistance	Δ Tc °C	WATER QUENCH	-	-
Dielectric Strength @ 6.35mm	ac-kV/mm ac V/mil	ASTM-D116	-	-
Dielectric Constant	1 MHz @ 77°F | 25°C	ASTM-D150	8	-
Dielectric Loss (Tan Delta)	1 MHz @ 77°F | 25°C	ASTM-D150	-	-
Volume Resistivity @ 77°F | 25°C @ 932°F | 500°C @ 1832°F | 1000°C	ohm-cm	ASTM-D1829	> 10^{14} - -	- - -

Table 4: Silicon Nitride properties.

- Burner nozzles, pilot and flare tips.
- Reactor vessel linings, bubble caps, and tuyeres.

Refractories, while not considered advanced ceramics, should receive mention here as they represent the highest volume use of ceramics in the heat-treat industry. Refractories are non-metallic materials having those chemical and physical properties that make them applicable for structures, or as components of systems, that are exposed to environments above 1,000°F (538°C) made up of all the materials previously mentioned as fillers or components of the mix. Refractory materials are used in furnaces, kilns, incinerators, power generators, and reactors. Refractories are also used to make crucibles, cores, and molds for casting glass and metals. The iron and steel industry and metal casting sectors use approximately 70 percent of all refractories produced.

Properties	Units	Test	Cordierite
Color			Orange - Tan
Density	g/cm^3	ASTM-C20	2.0
Water Absorption	%	ASTM-373	10
Gas Permeability	Atms-cc/sec	-	Porous
Flexural Strength (MOR)	MPa (psi x 10^3) @ 68°F | 20°C	ASTM-F417	66 (9.5)
Elastic Modulus	GPa (psi x 10^6) @ 68°F | 20°C	ASTM-C848	103 (15)
Poisson's Ratio	@ 68°F | 20°C	ASTM-C848	0.31
Compressive Strength	MPa (psi x 10^3) @ 68°F | 20°C	ASTM-C773	165 (24)
Hardness	R45N Gpa (kg/mm^2)	ROCKWELL 45N KNOOP 1000 gm	50 5.8 (590)
Tensile Strength	MPa (psi x 10^3) @ 77°F | 25°C	ACMA TEST #4	19 (2.7)
Fracture Toughness	MPa m$^{1/2}$ K_{Ic}	NOTCHED BEAM	-
Thermal Conductivity	W/m K @ 68°F | 20°C	ASTM-C408	2.5
Dielectric Strength @ 6.35mm	ac-kV/mm ac V/mil	ASTM-D116	10 (255)
Dielectric Constant	1 MHz @ 77°F | 25°C	ASTM-D150	5
Dielectric Loss (Tan Delta)	1 MHz @ 77°F | 25°C	ASTM-D150	7.0
Volume Resistivity @ 77°F | 25°C @ 932°F | 500°C @ 1832°F | 1000°C	ohm-cm	ASTM-D1829	10^{12} 10^6 10^8

Table 5: Cordierite properties.

ABOUT THE AUTHOR

CeraMaterials' Materials Science Engineer Jerry Weinstein has a Ph.D. in ceramic engineering from Rutgers University with more than 30 years' experience, 46 U.S. patents, and numerous publications and presentations. He has extensive experience working and consulting in fields such as advanced ceramics, graphite composites, heat treating, armor, aerospace, turbine engines, electronics, nano-composites, erosion/corrosion and whitewares. Jerry also consults outside projects through CeraGraphiSolutions.

D. SCOTT MACKENZIE, PH.D., FASM
SENIOR RESEARCH SCIENTIST–METALLURGY /// QUAKER HOUGHTON INC.

A discussion of proper racking, delaying onset of natural aging, and the effect of forming or straightening on the final aged part.

Heat treatment of aluminum IV: Handling distortion

After quenching, depending on the quenchant used, distortion of parts can occur. This is particularly true for water-quenched parts. Parts must be straightened. This is often much easier in the as-quenched condition before aging. However, there are certain things that must be understood to achieve straight parts. In this article, we will discuss a little about distortion in aluminum alloys, and how racking influences distortion. Secondly, we will discuss refrigeration of parts before they are straightened. Finally, we will discuss the act of straightening or forming in the as-quenched condition, and how properties are influenced.

RACKING OF PARTS

Of all the possible "defects" occurring during the heat treatment of aluminum, distortion during quenching is the most common. It is probably responsible for most of the non-value-added work (straightening) and costs associated with aluminum heat-treating.

Distortion during quenching is caused by differential cooling, and differential thermal strains developed during quenching. These thermal strains could be developed center-to-surface, or surface-to-surface. This differential cooling can be caused by large quench rates, so that the center is cooled much slower than the surface (non-Newtonian cooling) or by non-uniform heat transfer across the surface of the part.

Aluminum is more prone to quenching distortion than steel. This is because solution heat-treating temperatures are so close to the liquidus temperature. Aluminum exhibits less strength and greater plasticity than steel at the solution heat-treating temperature (or austenitizing temperature for steel). Much higher quench rates are necessary in aluminum to prevent premature heterogeneous precipitation occurring during quenching, and to maintain supersaturation of the solute.

In steel, there is a coupled phase transformation of austenite to martensite. This causes a 3 percent volume change during quenching. There is no coupled phase transformation in aluminum that can cause cracking or distortion. However, the coefficient of linear expansion of aluminum is approximately twice that of steel (2.38x10-5 mm/mm for aluminum compared to 1.12×10^{-5} mm/mm for steel). This causes much greater changes in length or volume as a function of temperature and increases the probability that distortion will occur.

Racking of the parts is critical. The parts should be fully supported, with the loads spread out over a large area, since the creep strength of aluminum is poor. The effect of this is illustrated in Figure 1. Parts should be wired loosely to prevent the parts from hitting each other during solution heat treatment. If wired too tightly, the wire could cut the parts. The use of pure aluminum wire minimizes this problem. Parts are often tied to steel racks for support.

If the parts are tied to the steel support too rigidly, the aluminum will grow at a much greater amount than the steel during heating. Upon cooling, the aluminum will contract more than the steel. Allowing movement of the aluminum by loosely attaching the parts to the rack will allow movement of the aluminum and reduce distortion.

Figure 1: Improperly supported aluminum forging resulting in gross distortion of flanges.

Alloy	Maximum delay time after quenching	Maximum storage time for retention		
		−12° C (10° F) max	−18° C (0° F) max	−23° C (−10° F) max
2014 2024 2219	15 minutes	1 day	30 days	90 days
6061 7075	30 minutes	7 days	30 days	90 days

Table 1: Typical time and temperature limits for refrigerated parts stored in the as-quenched condition.

Because of the poor strength of the heat-treated aluminum parts, distortion of the parts can occur as they enter the quenchant. Generally, parts should enter the quenchant aerodynamically to avoid distortion to the part before it even enters the quenchant. It should enter the quenchant smoothly — it should not "slap" the quenchant.

Racking a part so that it enters the quenchant smoothly also offers the benefit that it is more likely to have uniform heat transfer across the part. Distortion is more likely to occur because of horizontal changes in heat transfer than by vertical differences in heat transfer.

REFRIGERATION TO DELAY NATURAL AGING

Before natural aging occurs after solution treating and quenching, the ductility approaches that of the annealed condition. This allows

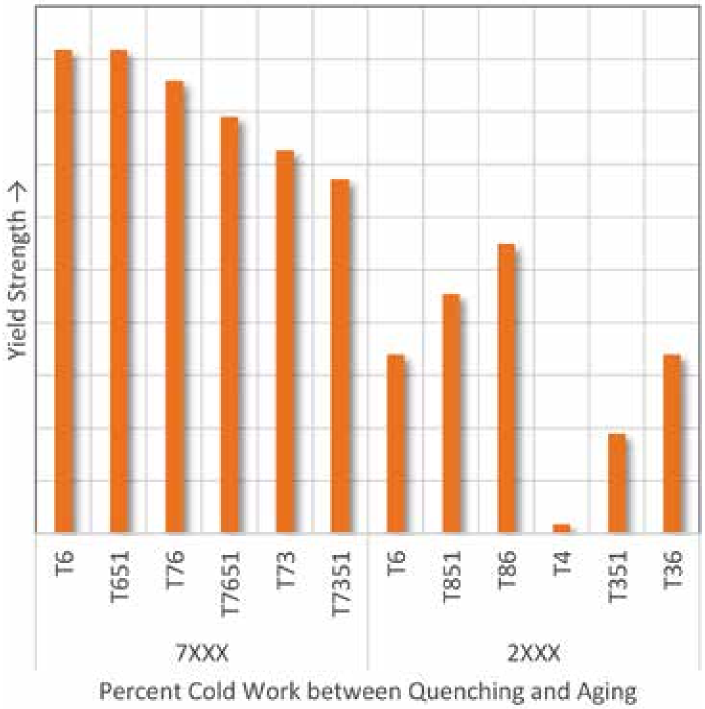

Figure 2: Schematic illustration of the effects of cold work after quenching on the strength of 2XXX and 7XXX alloys.

Additional Digits for T Tempers	Wrought Product Type	Stress Relief Process	Amount of Stretch
T_51X	Plate	Stretching	1-3%
T_51X	Rolled or cold finished rod and bar	Stretching	1-3%
T_51X	Die or ring forgings and rolled rings	Stretching	1-5%
T_510X	Extruded rod, bar, profiles, and tube	Stretching	1-3%
T_510X	Drawn tube	Stretching	0.5-3%
T_511X	Extruded rod, bar, profiles, and tube	Stretching	1-3%
T_511X	Drawn tube	Stretching	0.5-3%
T_52X	All products	Stretching	1-5%
T_54X	Die forgings	Restriking	–

Table 2: Additional digits used to designate stretch for wrought aluminum alloys.

forming of parts or straightening to correct warpage and distortion resulting from solution heat treating and quenching. Forming can be most readily accomplished immediately after quenching, but workload may not allow working to be completed before natural aging makes the parts difficult or impossible to form. In this case, it is common practice to refrigerate the parts quickly after quenching to sub-zero temperatures. Precipitation is temperature dependent, so it is possible to retard, or even prevent, natural aging by cooling the metal to low temperatures immediately after quenching. Typical time limits for alloys stored in the as-quenched condition are shown in Table 1 [1].

STRETCHING OR FORMING AFTER QUENCHING

Immediately after quenching, AQ Temper alloys are nearly as ductile as the "O" or annealed condition. Because of this, as-quenched alloys are often formed after quenching, but before artificial aging.

The effects of cold working on toughness after precipitation hardening are directly opposite for 2XXX and 7XXX alloys. Cold working after quenching improves the combination of strength and toughness in 2024 [2] and decreases the combination of strength and toughness in the overaged tempers. This is attributed to the precipitation of a fine distribution of S´ on dislocations. However, in 7050, cold working after quenching has the opposite effect [3]. This is attributed to the nucleation and preferential growth of coarse η´ on dislocations. This decreases the strength, without improving the toughness. This is shown in Figure 2.

Stretching of plate materials is generally performed to relieve the stresses induced from quenching. The amount of stretch varies but is generally in the range of 1 to 5 percent. Because the stretch plastically deforms the plate, many dislocations are introduced into the material. This plastic deformation causes the elastic stresses resulting from quenching to be redistributed into a less deleterious amount. Applying about 1-3 percent plastic deformation on the part generally causes this mechanical stress redistribution. This is accomplished by stretching of extrusion and plate, or by compression striking forgings. To designate the amount of stretch, additional digits are assigned after the basic temper designation. These are illustrated in Table 2. [4]

Forming of parts can serve two purposes — either to put the part into the proper geometry, or to correct distortion. Brake forming is often used to put sheet stock into simple shapes prior to aging. Hydroforming is nearly always performed when the part is either in the annealed condition or the as-quenched condition. Straightening of parts is usually performed in the as-quenched condition. The part is checked against a die, and the part is then straightened by either hammering or by bending the part to fit the die. This is a very time-consuming process that is avoided with the use of polymer quenchants.

CONCLUSION

In this short article, we discussed the causes of distortion in aluminum and the importance of proper racking methods. We also discussed the use of refrigeration to delay the onset of natural aging, so that straightening can be accomplished while the parts are in the soft as-quenched conditions. Finally, we discussed the effect of forming or straightening on the properties of the final aged part.

In the next article, we will talk about the mechanisms of natural and artificial aging. Should you have any questions regarding this article, or suggestions for additional articles, please contact the editor or myself.

REFERENCES

[1] D. S. MacKenzie, "Heat Treating Aluminum for Aerospace Applications," in METIF 2002, 7-11 May 2002, Brescia, Italy, 2002.

[2] J. E. Hatch, Aluminum: Properties and Physical Metallurgy, Metals Park, OH: American Society for Metals, 1984.

[3] H. J. Kolkman, W. G. t'Hart and L. Schra, "Quench Sensitivity of Airframe Aluminum Alloys," in Proceedings of the Conference on Strength of Metals and Alloys, August, 1988, Finland, 1988.

[4] J. C. Benedyk, "International Temper Designation System for Wrought Aluminum Alloys: Part II - Thermally Treated (T Temper) Aluminum Alloys," Light Metal Age, pp. 16-22, August 2010.

ABOUT THE AUTHOR

D. Scott MacKenzie, Ph.D., FASM, is senior research scientist-metallurgy at Quaker Houghton Inc. For more information, go to https://home.quakerhoughton.com/

JASON SCHULZE
METALLURGICAL ENGINEER /// CONRAD KASIK

Attend a PA Nadcap conference to learn how PRI governs the program. Read on to deepen your understanding of the benefits.

An argument in support of Nadcap

I think it is safe to assume that the majority of *Thermal Processing* readers have, in some capacity and at some point in their career, been exposed to Nadcap in either one or multiple commodities. Throughout my consulting career, I've had discussions regarding many aspects of the Nadcap organization as well as its process. These conversations can at times, turn negative. In this article I would like to present an argument in support of Nadcap.

HISTORY

Before explaining my argument, I feel it's appropriate to give some background on Nadcap's (formerly NADCAP) formation as well as its current mission.

It was identified in a conference in 1985 that redundant prime process audits conducted on process suppliers could be greatly reduced if they could find a way to consolidate the efforts. In 1990, SAE launched PRI as a separate nonprofit (501(c)(6) organization to govern Nadcap. In the beginning, Nadcap had conducted five NDT audits by the end of 1990. By 1994, Welding, Heat Treat, Materials Testing Laboratories, Chemical Processing, and Coatings were added as commodities. In 2002, Nadcap launched its business support software, eAuditNet. Now, Nadcap is spread through the Americas, Europe, and Asia and includes Transportation and Power Generation, Medical Devices, Nuclear (2011), as well as the institution of the MedAccred program (2014). Nadcap is based in Pittsburgh, Pennsylvania, but also has a European and Asia office as well. Alongside Nadcap, PRI has branched out in areas such as eQuaLified and eQuaLearn (I am a contracted Lead eQuaLearn Instructor). Nadcap has grown into an industry standard that, as far as I can see, isn't going anywhere.

THE CON ARGUMENT

Arguments I hear against Nadcap are, as an example, "it is a monopoly." I understand that the word "monopoly" is either associated with a competitive business monopolizing a market or simply the board game (maybe we'll see a Nadcap version soon). It is true, PRI/Nadcap is a monopoly, but remember, the intention was to centralize requirements and accreditation to achieve consistency in processing and quality systems, not to create a new product for American consumption that will become competitive in the market. There is no other way to accomplish this aside from establishing a monopoly. This seems logical to me. It would be like having multiple direct managers. You would receive conflicting requirements from each manager, causing any meager amount of consistency to disappear, and in the end, it would detrimentally affect your performance. We need to achieve quality through consistency and centralized requirements. Nadcap has achieved that.

Another argument against Nadcap is that suppliers who are receiving their Nadcap accreditation for the first time are doomed to fail. An article written by Christopher Paris, published September 7, 2018, states:

"First, just get it into your head that no matter how bulletproof you think your special process is, and even after you've conducted the mandatory self-audit beforehand, the Nadcap auditor is going to fail you on the first try. It's so prevalent, I am convinced it's hard-baked into some internal PRI procedure. The auditor will always find something wrong that requires a one-day follow up audit. Just be prepared for that; check your ego, and let them do it. Consider it a cost of doing business, and it won't be that expensive anyway. But you are not going to pass your audit on the first try. Consultants who tell you otherwise either don't have actual experience in this, or are just lying." [1]

Nadcap's operating procedures are public. Any Nadcap approved supplier or even someone who has gained access to eAudit.net and is not a supplier (yes, you can do this) can easily read the Nadcap operating procedures as they apply to both PRI staff and Nadcap auditors.

I realize this may seem as though it is an extreme example, but in conversations I have in which the other person is speaking negatively, this idea comes up often. Nadcap's operating procedures are public. Any Nadcap approved supplier or even someone who has gained access to eAudit.net and is not a supplier (yes, you can do this) can easily read the Nadcap operating procedures as they apply to both PRI staff and Nadcap auditors. In no procedure does it give a fail-first mandate to auditors. Even if there was a secret mandate that was unwritten, for the sake of the auditor's reputation and integrity, I don't know a single auditor who would follow such a secret mandate.

On another note, stating that you will, no matter how well you prepare, fail your first audit is just not the case. I have worked with countless potential suppliers, both commercial and captive (in-house) processors, who have gained Nadcap accreditation on the first try (even in heat treat). Of course, I am sure there are some who are simply not well prepared, but this should not be seen as a reflection of Nadcap or PRI; this is due to the potential supplier not being prepared in one way or another.

This same theory can translate to the notion that, no matter how well you prepare, you will receive a finding because the auditor "has to find something." Again, this is not the case. I've been through audits and received zero findings (again, yes, in heat treat). The irony behind this is that, a year later when performing an internal audit, I found two items that were missed that would have constituted two minor findings on the initial audit. Auditors are humans, too.

A PERSONAL POSITION

PRI and Nadcap, as well as the eQuaLearn team, have designed systems which allow both primes and suppliers to have input on the checklist requirements as well as handbooks. When I try and imagine performing this task, I can't see any easy route. Organizing prime requirements and industry standard requirements all the while filtering "experts'" opinions out of the mix … it must have been a task that seemed to have no light at the end of the tunnel.

If you have ever been to the annual PA Nadcap conference you will gain, at the very least, a small amount of respect for how PRI governs the Nadcap program. Anyone in the room has an opportunity to voice their concerns and questions and they are addressed, if not immediately in that setting, they are documented and addressed at a later time. PRI staff engineers are also available via email to answer questions, which they do often. Their emails can be found on the contacts tab at the top right-hand side of the eaudit.net page.

SUMMARY

PRI manages a monster that is ever-changing and growing. This is a tough task. It's very easy to voice armchair opinions, but ask yourself this: Is it PRI that does not govern Nadcap well, or is it suppliers who are simply not prepared for their audits? PRI may have areas they could improve on, but all organizations do. Areas where suppliers feel PRI could improve should be voiced in the annual meeting.

I commend PRI for its governance of Nadcap. The institution of eQuaLearn is also a step forward as you can enroll in courses, sponsored by PRI, with content that is reviewed by PRI staff engineers; I can't think of anything further PRI could have done to help suppliers navigate the gauntlet.

REFERENCE

[1] www.oxebridge.com/emma/new-to-nadcap-audits-heres-what-to-expect

ABOUT THE AUTHOR

Jason Schulze is the director of technical services at Conrad Kacsik Instrument Systems, Inc. As a metallurgical engineer with 20-plus years in aerospace, he assists potential and existing Nadcap suppliers in conformance as well as metallurgical consulting. He is contracted by eQualearn to teach multiple PRI courses, including pyrometry, RCCA, and Checklists Review for heat treat. Contact him at jschulze@kacsik.com.

This article first appeared in the January 2019 issue of Thermal Processing.

ELECTRICAL HEATING IN VACUUM APPLICATIONS

Vacuum drying is a low-pressure operation used to remove moisture from a substance. (Courtesy: BriskHeat Corporation)

Heat and vacuum can be used together to process materials that could not otherwise be accomplished.

By EDYE S. BUCHANAN

Applying electrical heat to materials under vacuum can be an important manufacturing process to ensure product quality when drying, high-purity processing or other vacuum heating is required. The use of vacuum promotes off-gassing and reduces the boiling point of trapped liquids. Unfortunately, vacuum alone may cause liquid evacuating from the material or part to freeze. What remains are ice particles, which are not easily evacuated from the system.

Using heat and vacuum in tandem provides improved results compared to either process used separately. Applying heat with vacuum prevents ice formation and decreases the heat needed to sufficiently remove moisture and volatile compounds from parts. Three common applications using heat/vacuum combination include: vacuum drying, vacuum bakeout, and vacuum heating for metal processing. To regulate heat applied in any vacuum application, a PID temperature controller is required to more accurately control the heating process.

VACUUM DRYING

Vacuum drying is a low-pressure operation used to remove moisture from a substance. This is used when higher temperatures may result in hazardous situations or potential damage to the product. The boiling point of liquids is reduced when subjected to vacuum pressure. A combination of vacuum and heat is used to reach the vapor pressure of water. This causes the water to boil into a gaseous state. For example, at atmospheric pressure 760 mm Hg (14.7 psi), water boils at 100°C (212°F). Under a vacuum of 150 mm Hg (2.89 psi), water boils at 60°C (140°F). The vacuum system, including pipe headed with individual cloth jackets (Figure 1), evacuates the gases from the chamber, preventing it from condensing and rewetting the product while cooling. Products processed with vacuum drying include:

- Pulp and paper products.
- Pharmaceuticals.
- Power or granulated minerals.
- Food products.
- Plastic parts.
- Resin parts.

Vacuum drying in a vessel requires a heating system designed with sufficient wattage and insulation to increase the temperature from ambient to that required for off-gassing. Not only does vacuum drying remove trace amounts of moisture, but it allows batch processing to be done, taking less time compared to conventional drying methods.

HIGH AND ULTRA-HIGH VACUUM BAKEOUT

High or ultra-high vacuum applications as well as other applications using high-purity parts necessitate a vacuum bakeout process. During manufacturing, many components will be left with some type of unwanted residue. This can be moisture in compounds, cutting oils, solvents, dust, or corrosion. Conventional cleaning methods should be used to remove contaminants. Vacuum bakeout elevates the surface cleaning efficiency by eliminating microscopic particles. It is a necessary process in which failure to remove the impurities will contaminate the product or spoil the vacuum. While water vapor

Figure 1: Heated piping reduces the risk of condensate in vacuum systems.

absorbed from the atmosphere is the most common contaminant, oil particles from pumps and dust accumulated during assembly must be removed. Without careful handling, fingerprints left on surfaces can also be problematic.

How can even microscopic particles ruin a vacuum? As heat and vacuum are applied to the part, particles are extracted from the surface and move within the vacuum chamber. This movement creates pressure that works against the vacuum. Successive flushing of the chamber evacuates loose particles with vacuum pressures of $<10^{-10}$ mbar. Figure 2 shows a custom cloth heating jacket with temperature controller designed for a vacuum chamber.

Applications requiring high-purity vacuum bakeout include:

- Particle acceleration (particles at 99.99 percent the speed of light).

- High-energy physics.
- Radiation therapy.
- Surface coating.
- Deposition and etch (semiconductor manufacturing).
- Gas delivery.
- Mass spectrometry.

The process engineer has three things to consider when designing a vacuum bakeout system:

1. Bakeout temperature.
2. Temperature distribution.
3. Time at temperature.

Ideal bakeouts may require temperatures of 300 to 400°C (572 to 752°F), which is too high for extruded silicone rubber tapes. Fiberglass insulating tapes and high-temperature insulators can be used. At temperatures above 300°C (572°F), yarn on the tape may become brittle and, once removed, cannot be reused. During vacuum bakeout, temperature distribution is more critical versus a drying application. Cold spots on the surface of objects being baked may not expel impurities, resulting in a poor vacuum. Temperature uniformity can be achieved by using a heated cloth jacket. Heating tapes, shown green in the photo, are sewn into cloth jackets providing heat to surfaces that might be difficult by other solutions (Figure 3).

VACUUM HEATING FOR METAL PROCESSING

Vacuum heating can be performed by placing products or vessels within a vacuum oven fabricated from stainless steel with openings for inserting items to be processed and for the vacuum system. Ovens can be small chambers as the one using band heaters to anneal graphite electrodes (Figure 4) large cylindrical shapes that fit over coils of steel. Openings should be designed to prevent outside air infiltration when the oven is closed. Non-destructive testing and inspections must be used to ensure there are no leaks in the system.

Heating tapes may be an option and should be wrapped carefully around the chamber to contact as much surface area as possible. Silicone surface heaters can be used for application temperatures of 204 to 232°C (400 to 450°F). These can include insulating foam up to 2.54 mm (1") thick with pressure sensitive adhesive for installation. For higher temperature applications up to 593°C (1,100°F), cloth heating blankets are available. After securing heaters around the chamber, insulation should be applied sufficient to maintain a touch-self temperature, typically 48 to 60°C (120 to 140°F). A durable cover may need to be placed over the insulation to preserve the integrity of the material.

Figure 2: Multi-zone heating blanket. (Courtesy: BriskHeat Corporation)

Vacuum heating can be used in many metal-processing applications. Processing under vacuum reduces the possibility of impurities during the melting and casting of alloys. Purity is also very important in the manufacturing of powered metals used for 3D printing. Carburization, a process adding carbon atoms to the top layers of steel for surface hardening, is typically performed at 900 to 950°C (1,652 to 1,742°F). It can also be performed at temperatures below 600°C (1,112°F) when under vacuum. Other heat treatments such as tempering and annealing allow for heating to lower temperatures and cooling of metals without the risk of impurities or oxygen.

CUSTOMIZED HEATING AND INSULATING OPTIONS

Heat can be applied using silicone or fiberglass heaters and require

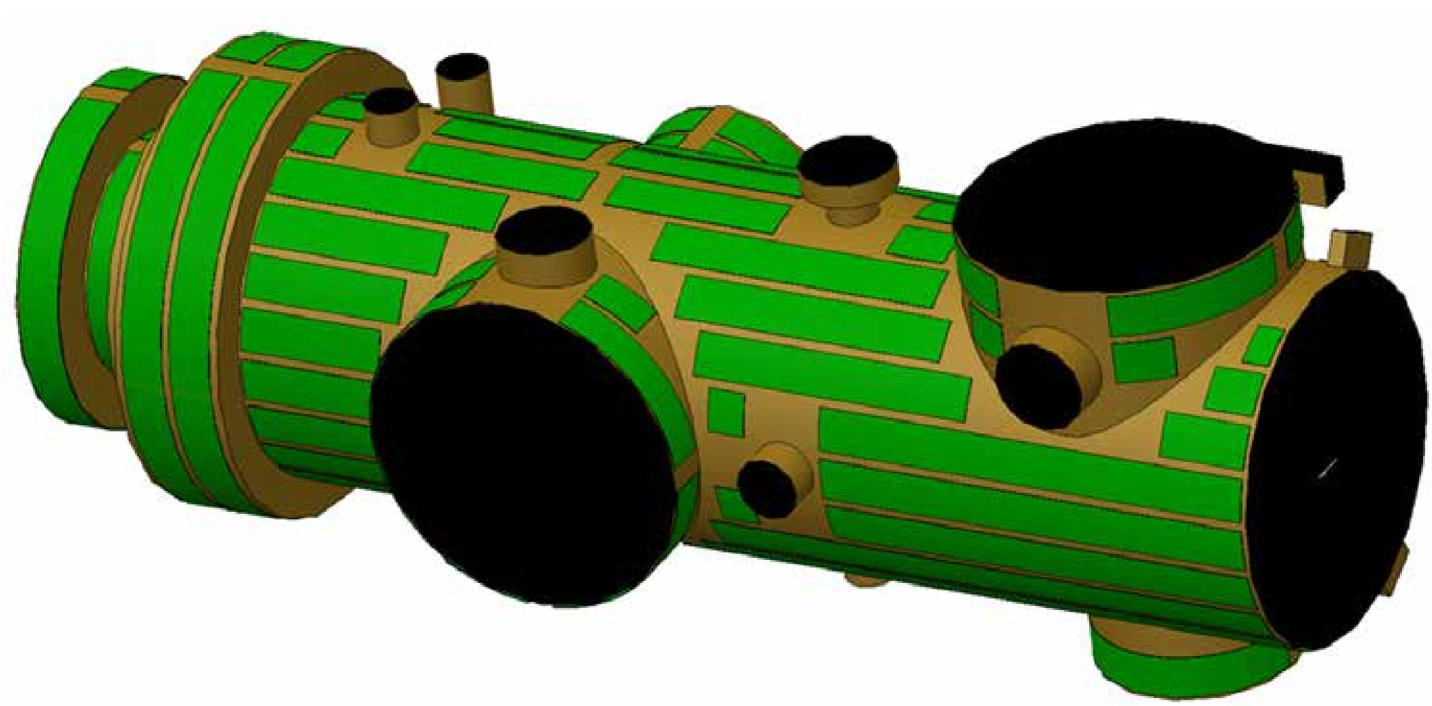

Figure 3: Heated tape integrated into an insulated cloth jacket. (Courtesy: BriskHeat Corporation)

separate insulation. Custom silicone blankets may be available with special contours or cutouts to provide better temperature uniformity than what may be available from off-the-shelf solutions.

Cloth insulating jackets are the best way to prevent heat loss and reduce cold spots. These are manufactured with durable material covers. Fiber insulating blanket, typically available in rolls, is not recommended as these are often not capable of being wrapped sufficiently tight enough to promote temperature uniformity. Fiber insulation incorporates binders in its construction that release fumes when heated, are in general less durable, and any loose fibers produced during installation create a safety hazard if proper PPE is not used.

Cloth heating jackets are designed similarly to insulating jackets. Resistance wires are sewn to the interior liner, covering more surface area than tapes and providing superior temperature uniformity. The wires are covered with an insulating fiber and retained by a top cloth cover. Samox^{TM} cloth can be incorporated into the liner, meeting Class 100 environments with exposure temperatures up to 593°C (1,100°F). Fiber insulation between the wires and the outer cover provides a safe and cool-touch surface meeting the SEMI S2 standard. BriskHeat is one of several companies that provides insulators and heating jackets to fit a variety of valves and pumps sold by popular high vacuum component manufacturers.

TEMPERATURE CONTROL

A variety of temperature controllers is available for use with heating tapes and cloth heating jackets. The more critical the temperature and complex the system, the more important the choice. Most vacuum systems use a central monitoring system (CMS) to control the heat and vacuum. Control of each individual heater provides for the best temperature uniformity, and cloth jackets can be purchased with integrated control modules and sensors. Controllers can use PID (proportional-integral-derivative) or on/off control. PID has a feedback loop that can continuously modulate the heating circuit as opposed to the current to the heater being either on or off.

CONCLUSION

Heat and vacuum can be used together to process materials that could not otherwise be accomplished. Vacuum drying can be completed at lower temperatures and in less time, which reduces cost. High and ultra-high vacuum removes even the most microscopic impurities from surfaces when applications require high purity for consistent results. As new metal alloys are developed and metallurgical processes required to enhance properties, vacuum heating provides repeatable product quality. No matter what the application, insulation and temperature controllers should be appropriate for the heaters selected. There are a variety of off-the-shelf solutions available; however, custom designed heaters and insulators can provide superior performance. A qualified heating company can be consulted for application support.

ABOUT THE AUTHOR

Edye Buchanan is a sales strategist at BriskHeat Corporation. She uncovers new technologies and applications in industrial surface and immersion heating and temperature control markets. Applications include thermal processing and insulation, composite manufacturing and repair, and high vacuum. Buchanan's more than 30 years of experience in manufacturing has focused on design engineering, project management, and marketing. Buchanan holds a Bachelor of Science from Kent State University and is a Certified Manufacturing Technologist. She serves on the Board of Directors for SME (the Society of Manufacturing Engineers).

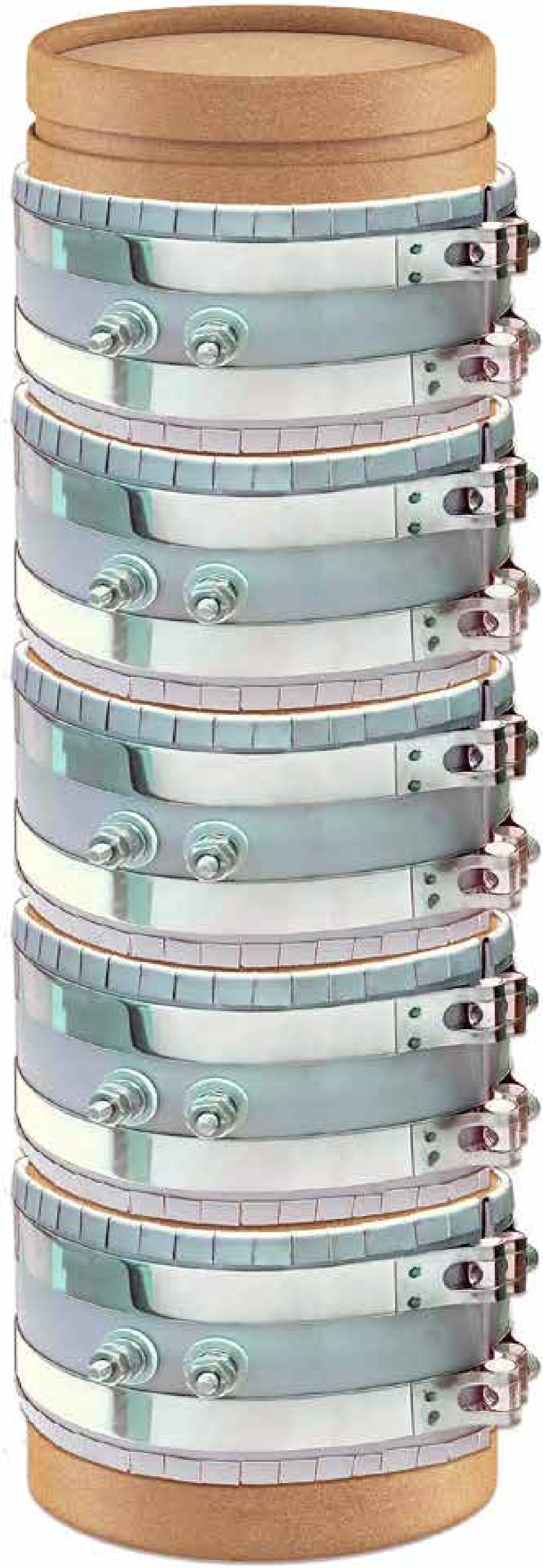

Figure 4: Band heaters around a ceramic kiln used for annealing graphite rods. (Courtesy: BriskHeat Corporation)

CAN SUB-ZERO TREATMENT AT MINUS-75°C BRING ANY BENEFITS TO TOOL MANUFACTURING?

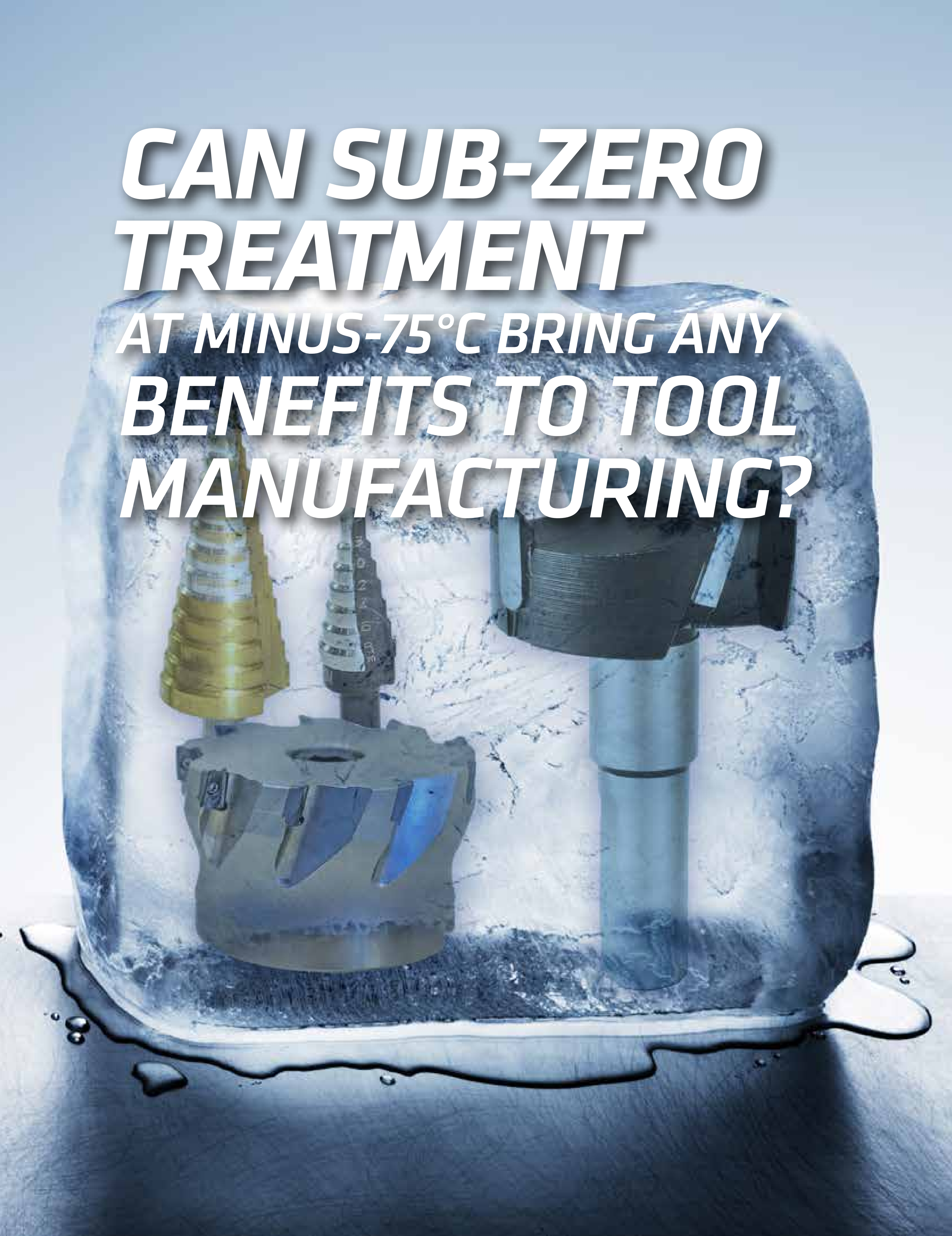

This paper focuses on an in-depth description of the results obtained with the sub-zero treatments of Vanadis 6 steel at a temperature of minus-75°C.

By MARTIN KUSÝ, LÝDIA RÍZEKOVÁ-TRNKOVÁ, JOZEF KRAJČOVIČ, IVO DLOUHÝ, and PETER JURČI

Vanadis 6 ledeburitic tool steel was subjected to sub-zero treatment at minus-75°C for different durations and for different subsequent tempering regimes. The impact of these treatments on the microstructure, hardness variations, and toughness characteristics of the steel was investigated. The obtained results infer that the retained austenite amount was reduced to one fourth by sub-zero treatment (SZT), and the population density of add-on carbides was increased by a factor of three to seven, depending on the duration of SZT. Tempering always reduced the population density of these particles. A hardness increased by 30 to 60 HV10 was recorded after sub-zero treatment, but tempering to the secondary hardness peak induced much more significant hardness decrease than what was established in conventionally quenched steel. The flexural strength was not negatively influenced by sub-zero treatment at minus-75°C while the fracture toughness tests gave worse values of this quantity, except the case of steel tempered to the secondary hardness peak.

1 INTRODUCTION

In conventional heat treatment of tools made of high-alloyed Cr and Cr–V ledeburitic steels, the material is gradually heated to the austenitizing temperature (recommended by the steel manufacturers), held there for prescribed time, and cooled down rapidly to room temperature. Afterwards, the steels should be subjected to tempering immediately to prevent the retained austenite stabilization and to induce transformations leading to the achievement of final properties of tools or components.

Ledeburitic steels are commonly used as tool materials for cold-work applications. In order to generate high abrasive wear resistance, they contain a high amount of carbide phases embedded in a metallic matrix. On the other hand, these carbides, together with high overall steel hardness, deteriorate the material resistance against crack initiation/propagation, expressed by the fracture toughness K_{IC}. Also, the flexural strength of ledeburitic steels, which is often also taken as a measure of resistance against crack initiation for brittle materials, manifests relatively low values. Moreover, conventionally produced ledeburitic steels are cast and afterwards hot formed. As a consequence, they contain band-like carbides, thus they suffer from anisotropy of key mechanical properties [1].

Sub-zero treatment is defined as a supplementary process to conventional heat treatment. Unlike conventional heat treatment (CHT), it is a process where the tools or components are immersed into a suitable cryo-processing medium, stored there for a pre-determined time (usually in 10s of hours), and re-heated to room temperature. Research works conducted on the application of this kind of treatment have shown that sub-zero treatments provide extra benefits to the tooling industry such as increased hardness [2,3], better wear performance [3,4], and improved dimensional stability of products [5].

According to recent studies, the following crucial microstructural changes are responsible for these benefits:

1. Considerably reduced retained austenite (γ_R) amount [2,6-9].

2. Refinement of the martensite along with an enhanced number of crystal defects such as dislocations and twins inside martensitic domains [7,9,10].

3. Enhancement of number and population density of small globular carbides (SGCs) [2,3,7,8,11,12].

4. Acceleration of the precipitation rate of nano-sized transient carbides [11-15].

However, the impact of sub-zero treatments on the toughness characteristics (fracture toughness, flexural strength, and impact toughness) is controversial as Table 1 illustrates.

The question of an optimal regime of sub-zero treatments is still under debate. In the "pioneer age" of this technique, it was believed within the professional community that the benefits of sub-zero treatments are based only on the reduction of retained austenite amount. Therefore, the temperatures of about minus-75°C were widely used in laboratory and industrial practice. Lower temperatures were not accepted for the treatments since their use often led to premature failure of tools due to thermal shocks associated with the use of very low temperatures. Treatment at the boiling temperature of liquid nitrogen (minus-196°C) was introduced into industrial practice much later, when the devices enabled could carry out well controlled cooling down to such low temperature.

Other sub-zero treatment temperatures were suggested only by a very limited number of researchers. Reitz and Pendray and Gavriljuk et al., for instance, suggested the temperature of minus-140°C [24,25]. Recent studies dealing with thorough analysis of microstructure and toughness of the Vanadis 6 steel treated in this way gave very promising results [22,26]. Alternatively, there were attempts and/or suggestions with the use of the temperature of boiling helium (minus-269°C) [13,27]. However, the treatment temperature of minus-75°C also deserves attention since one can expect the phenomena being responsible for earlier mentioned ameliorations in properties would proceed faster at minus-75°C than at lower temperatures. Also, practical experiences indicated the extent of "extra" wear performance (or other property), which can be gained by the use of SZT at minus-96°C (as compared with treatments at minus-75°C) depends on the material chemistry. For instance, the wear performance of AISI D2 steel was improved by a factor of 2.59 by the treatment in liquid nitrogen (as compared with treatment at minus-75°C), while only an improvement by a factor of 1.39 was recorded for CPM 10-V steel (steel with high vanadium content) [24].

This paper is thus focused to an in-depth description of the results obtained with the sub-zero treatments of Vanadis 6 steel at the temperature of minus-75°C, and to their careful discussion. Microstructural changes are presented, and they are related to the hardness, flexural strength, and fracture toughness of examined steel. The obtained results are also compared to what was obtained by treatments at temperatures minus-140, minus-196, and minus-269°C, respectively.

Steel	Treatment	Quantity	Description	Reference
AISI D2	–70, –100, –130, and –196 C, tempering at 200 C	Impact toughness	Considerable reduction, extent of reduction depends on both the austenitizing temperature (better toughness is achieved at lower austenitizing temperature) and SZT temperature (–70 C produces the lowest values)	[16]
AISI D2	–196 C/16 h, tempering at 170 or 450 C	Impact toughness	Considerable reduction, degree of reduction is much higher than the improvement of hardness	[17]
AISI D2	–196 C/20 h	Impact toughness	Reduction after low-temperature tempering but improvement after tempering to the secondary hardness	[18]
AISI D2	–196 C/36 h, –75 C/5 min –125 C/5 min, tempering at 210 C	Fracture toughness	Significant reduction after SZT at either –75 or –125 C, moderate reduction after SZT at –196 C	[19]
Vanadis 6	–196 C/4 or 10 h, –90 C/4 h, tempering twice at 530 C	Flexural strength, fracture toughness	Marginal effect on flexural strength but slightly positive effect on fracture toughness	[20]
Vanadis 6	–196 C/17 h, tempering 170–530 C	Flexural strength, fracture toughness	• Marginal effect on flexural strength in low-temperature. • Tempering range, improvement in normal secondary hardening temperature range. • Worsening of fracture toughness except tempering to the secondary hardness.	[21]
Vanadis 6	–140 C/17 h, tempering at 170–530 C	Flexural strength, fracture toughness	• Slight improvement of flexural strength at low tempering temperatures but almost no effect after tempering at 450 C and above. • Improvement of fracture toughness after high temperature tempering but slight deterioration after tempering within the 170–450 C range	[22]
AISI D3	–196 C/12, 24 or 36 h, tempering at 150 C	Impact toughness	Significant reduction, the reduction is more pronounced with increasing the duration of SZT	[23]

Table 1: Toughness and fracture toughness of differently sub-zero treated ledeburitic steels — an overview of the obtained results to date.

2 EXPERIMENTAL

The powder metallurgy (PM) tool steel, Vanadis 6, with nominal composition (in wt%) 2.1 C, 1 Si, 0.4 Mn, 6.8 Cr, 1.5 Mo, 5.4 V, and Fe as a balance was selected for the examinations. Due to the PM technique used for steel manufacturing, the material is free of macro-segregations and also of carbide bands and manifests high degree of isotropy. This makes it possible to disregard the orientation in sample manufacturing. The initial microstructure was soft-annealed with a hardness of 272 HV10.

The specimens were machined to a net-shape and subjected to the heat-treatment schedules. Conventional heat treatment consisted of gradual heating up to the austenitizing temperature of 1,050°C, holding at that temperature for 30 minutes to enable the dissolution of carbides and austenite homogenization, which was followed by room temperature quenching by using cold nitrogen gas. Then, one set of specimens was separated and subjected instantly to tempering treatments. The other specimens were moved to a cryogenic system and subjected to sub-zero treatments at the temperature of minus-75°C and for different durations prior to tempering.

In sub-zero treatments, room-temperature quenched specimens were cooled down to minus-75°C, at a controlled cooling rate of 1°C/min, stored at the lowest temperature for predetermined duration (4, 10, 17, 24, or 48 hours), and re-heated by a heating rate of 1°C/min to room temperature. Immediately after the specimens reached room temperature, they were moved to the tempering furnace where they were tempered in an atmosphere of pure technical nitrogen. Tempering consisted of two cycles (2 + 2 hours), at temperatures in the range 170-530°C. However, the tempering temperature of 600°C was added to the experiments with flexural strength in order to verify the behavior of this mechanical quantity at tempering temperature located beyond the secondary hardness peak.

A NETZSCH DIL 402 C dilatometer (Netzsch, Selb, Germany) was used within the temperature range of 20 down to minus-150°C in order to estimate the martensite finish temperature of the Vanadis 6 steel austenitized at given austenitizing conditions.

The specimens for microstructural examinations were prepared using standard metallographic grinding by a set of abrasive papers (with a grit of 180, 320, 600, and 1,200) and polishing (by using the 9, 3, and 1 μm diamond suspensions). Then, the specimens were etched with Villella-Bain reagent (5 ml hydrochloric acid, 1 g picric acid in 100 ml of ethanol) for 10 seconds. For the material microstructure examinations, a JEOL JSM 7600 F scanning electron microscope (SEM, Jeol Ltd., Tokyo, Japan), operating at a 15 kV acceleration voltage was used. Microstructural examinations were coupled with energy dispersive spectrometry (EDS) by using an EDS detector (Oxford Instruments, plc., High Wycombe, UK). SEM micrographs were acquired in a combined 50:50 detection of secondary electrons and backscattered electrons (BE). The reason was that the material contains eutectic carbides (ECs), secondary carbides (SCs), and small globular carbides after application of the earlier mentioned heat-treatment schedules. It has been proven recently that the ECs are represented by vanadium-rich (more than 50 wt%V) MC particles, while the SCs are the

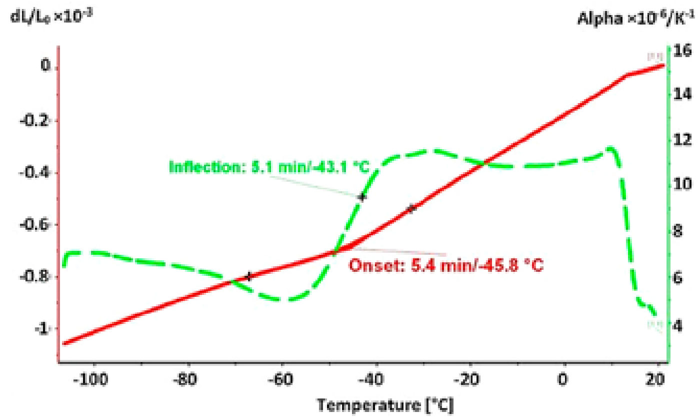

Figure 1: Dilatometry of Vanadis 6 steel after austenitizing at 1,050°C for 30 minutes, quenching to 20°C, and cooling from 20°C down to minus-110°C with a cooling rate of 10 K min^{-1}.

M_7C_3 particles (with a high percentage of chromium), and that SGCs were determined to be alloyed cementite [7]. This made it possible to clearly differentiate between the ECs on the one side and the SCs (and the SGCs) on the other side by strong differences in BE yield. Unfortunately, this categorization fails in differentiation between SCs and SGCs as their BE yield is very similar. Therefore, the classification based on the particle size was adopted to distinguish the ECs and the SGCs; the carbides finer than 0.5 μm were considered as the SGCs while the coarser ones as SCs.

Determination of population density of carbide particles (categorized as above-described) was carried out on 25 randomly acquired SEM micrographs for each specimen. Standard magnification for acquisition of SEM images was 3,000×. For better identification of SGCs, additional SEM micrographs at a magnification of 7,500× were recorded because some of these particles had a size well below 100 nm. The acquisition of SEM images was coupled with EDS mapping of chromium and vanadium in order to clearly differentiate between the carbides, as mentioned earlier. The mean values and the standard deviations of the obtained data were calculated.

The phase constitution of differently heat-treated specimens was determined by using X-ray diffraction (XRD, Philips Analytical B.V., Almelo, The Netherlands) technique. A Phillips PW 1710 diffractometer with filtered $Co_{K\alpha}$ characteristic radiation was used for this purpose. The diffracted radiation was registered within a two-theta angle range of 30-127 degrees. The retained austenite amounts were determined following the appropriate ASTM E975-13 standard [28], taking the characteristic peaks of both the martensite (α´) and the austenite (γ), namely (200)α´, (200)γ, (211)α´, and (220)γ into the consideration. As reported recently [2,7], however, these peaks are often superimposed by the characteristic peaks of carbides, which might influence the accuracy of the obtained results negatively. Therefore, the analyses were coupled with Rietveld refinement of the obtained X-ray spectra before computing the retained austenite amounts.

Hardness of differently heat-treated specimens was measured by using a Vickers indentation technique at a load of 98.1 N (HV 10) following the appropriate Czech standard [29]. A ZWICK 3212 hardness tester (Zwick-Roell, Ulm, Germany) was used. The distance between two adjacent indents was kept minimum 5 mm, and the dwell time used for each indent was 15 seconds; 10 measurements were done for each specimen. Then, both the mean values and standard deviations of measured values were calculated.

10 by 10 by 100 mm bar specimens were used for flexural strength determination. Prior to measurements, the specimens were polished to a final surface roughness, R_a, between 0.05 and 0.07 μm. This step is very important to obtain reliable results because it is known that the surface finish plays an important role in this type of measurement, and differences in surface finish (in microns of R_a) can influence the obtained flexural strength values within the range of hundreds MPa [30]. An Instron 8862 test device (Instron, Norwood, MA, USA) was used. Specimens were tested in a three-point bending configuration at a loading rate of 1 mm/min, until the moment of fracture. The distance between loading roller supports was 80 mm. The flexural strength R was calculated according Equation 1 (following the appropriate Czech standard [31])

$$R = \frac{3FL}{2bh^2}\ [\mathrm{MPa}] \qquad \textbf{Equation 1}$$

where F represents fracture force (maximum load on the load–deflection trace), L is distance of roller supports in three-point bending, b is the specimen thickness, and h is the specimen height (dimension in the direction of the acting load). In addition, the total work of fracture, W_{of}, and the plastic part of the work of fracture, W_{pl}, were evaluated from the corresponding area below the measured load-deflection (load displacement) curve.

Reliable evaluation of fracture toughness of materials by plane strain fracture toughness requires prior fatigue pre-cracking of the specimens in order to achieve a sharp and reproducible crack tip geometry for testing. Therefore, pre-cracked specimens with 10 by 10 by 55 mm dimensions were used for fracture toughness determination in the current work. Pre-cracking the samples was carried out after the heat treatment. A resonance frequency machine Cracktronic 8024 (Russenberger Prüfmaschinen AG, Neuhausen am Rheinfall, Switzerland) was used for this purpose, and the specimens were loaded in four-point bending configuration. The crack development was monitored on both sides of the sample using a digital long-distance microscope. Both the pre-crack preparation and the testing were carried out at room temperature following the ISO 12137 standard [32]. In testing, the specimens were loaded in three-point bending with a roller span of 40 mm and at a loading rate of 0.1 mm/min. An Instron 8862 machine (Instron, Norwood, MA, USA) was used. Specimen deflection was measured by means of an inductive transducer integrated directly into the loading axis. Five samples were tested for each investigated heat-treatment (SZT, tempering) condition.

Fracture surfaces were analyzed by using the scanning electron microscope JEOL JSM 7600 F. SEM micrographs were acquired in the secondary electron detection regime at different magnifications enabling a study of the micro-morphology of fracture surfaces. Particular attention has been paid to the role of carbide particles in the fracture propagation.

3 RESULTS AND DISCUSSION

The change in the length of the Vanadis 6 specimen after quenching from 1,050°C down to 20°C and immediate moving to the dilatometer, where the material was cooled down from 20°C to minus-110°C is presented in Figure 1.

The onset at the relative length curve is located at minus-45.8°C. The inflection at the linear expansion coefficient curve is at minus-43.1°C. From these two values it can be summarized that the critical M_f temperature of the Vanadis 6 steel lies at approximately minus-45°C, it is thus higher than the selected sub-zero treatment temperature.

SEM micrographs in Figure 2 show the microstructure of Vanadis 6 steel in the conventionally heat-treated state (a), and after subsequent SZT at minus-75°C for different durations (b-f). The matrix and different carbide particles are the main microstructural constituents of the steel, irrespectively to the heat-treatment schedule used. The matrix is mainly martensitic, with a certain amount of retained austenite. The retained austenite is in-between the martensitic laths as SEM micrograph in Figure 2a illustrates. The carbide particles are the eutectic carbides, the secondary carbides, and small globular carbides. The number and population density of both the ECs and the SCs are nearly constant within the range of the heat-treatment schedules used. Alternatively, the number and population density of SGCs change with the duration of SZT; they increase substantially up to the 10-hour duration of SZT in Figure 2b and 2c where the maximum population density of 233×10^3 mm^{-2} was achieved (Table 2), and then decrease, Figure 2d-f.

It is shown in Table 2 and in Figure 3 that tempering treatment always induces a reduction of population density of SGCs, despite that their population density remains two- to three-fold higher than what is produced by conventional heat treatment. Finally, it should be mentioned that SZT does not modify the amounts and population densities of ECs and SCs in Vanadis 6 steel as reported recently [7,12]. The reason is that these carbides are stable up to much higher temperatures and thus neither the SZTs nor the tempering modify their quantitative characteristics.

A series of high-magnification SEM micrographs in Figure 4 depicts the microstructural alterations of sub-zero treated (at minus-75°C) steel with increasing the tempering temperature. The as-sub-zero treated material microstructure contains the matrix formed by the martensite and retained austenite and eutectic, secondary, and small globular carbides, Figure 4a. Tempering treatment modifies the material microstructure as follows: The matrix manifests more pronounced sensitivity to the etching agent, Figure 4b-e. This is reflected by extensive roughening of the originally smooth metallographic surface, and thus by lowered distinctness of originally clearly visible matrix microstructural features (martensite laths, retained austenite, grain boundaries, etc.) obtained by austenitizing, quenching, and sub-zero treatments, compare with Figure 4a. Mentioned changes can be ascribed to extensive precipitation of nano-sized carbides. These carbide particles become visible after tempering at 450 or 530°C, as tiny elongated formations in Figure 4d and 4e. At the same time, the retained austenite disappears from the microstructure because it was decomposed into either "secondary" martensite or bainite during the cool down from the tempering temperature. Last but not the least, it should be noticed the population density of both the ECs and the SCs are nearly unaffected by tempering while the population density of SGCs decreases with tempering treatment, compare Figure 4a with micrographs in Figure 4b-e and see also Table 2. It should be noted that similar microstructural development was detected also for the steel after SZT at minus-75°C for other (shorter or longer) durations.

The dependence of the retained austenite amount on the tempering temperature for specimens after sub-zero treatment at minus-75°C for 17 hours is in Table 3. The amount of γ_R was 7.6 ± 0.4 vol% in the prior-to-tempering state. Tempering at low temperatures reduces the γ_R amount only moderately. In contrast, tempering at higher temperatures results in either the significant reduction (450°C) or in the almost complete removal of the retained austenite.

The γ_R amount in CHT specimens was about 20 vol% as reported recently [7,12]. The obtained results imply the SZT at minus-75°C reduces the γ_R amount to approximately one third as compared with the room temperature quenching. At the same time, however, it is worth noting that treatments at minus-140 or minus-196°C act more effectively in reduction of retained austenite; the γ_R amounts were determined 4.3 and 2.1 vol% for steel that was SZT at minus-140 and minus-196°C, respectively [7,12,26].

The prior-to-tempering hardness for conventionally (room temperature) quenched Vanadis 6 steel was 875 ± 16 HV10 in Figure 5. The

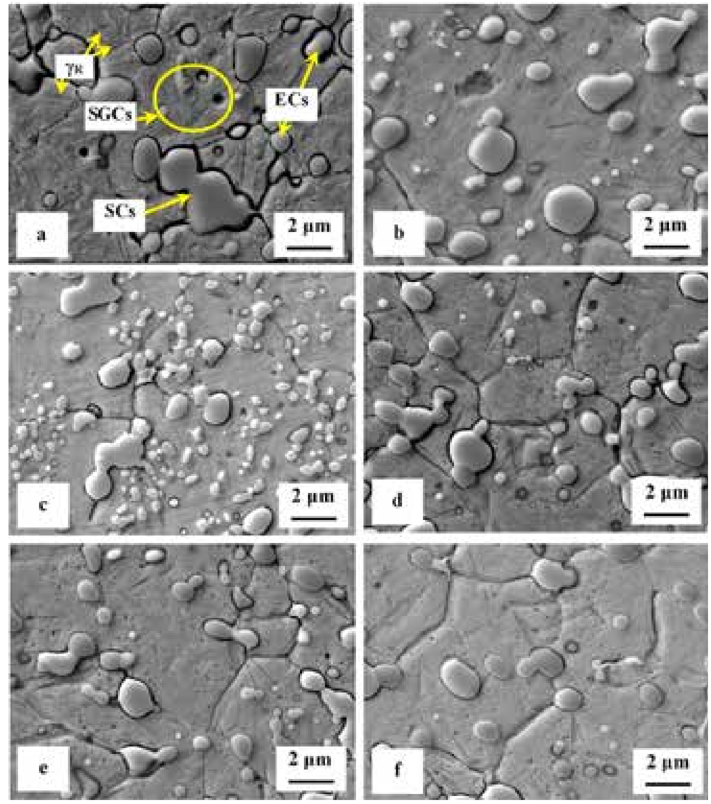

Figure 2: SEM micrographs showing the microstructure of no-tempered steel after conventional heat treatment (a), and after SZT at minus-75°C for 4 h (b), 10 h (c), 17 h (d), 24 h (e), and for 48 h (f).

Duration of SZT [h]	Tempering Temperature [C] No.	170	330	450	530
CHT	**38.7**	**33.5**	**35.3**	**47.6**	**37.4**
4	**171.6**	**119.4**	**116.1**	**107.9**	**95.4**
10	**233.2**	**125.6**	**97.0**	**84.5**	**73.5**
17	**136.9**	**121.9**	**101.7**	**103.0**	**93.3**
24	**121.8**	**104.6**	**84.8**	**73.7**	**69.2**
48	**119.8**	**115.6**	**115.4**	**106.0**	**79.5**

Table 2: Determined values of population density of small globular carbides for differently sub-zero treated and tempered specimens.

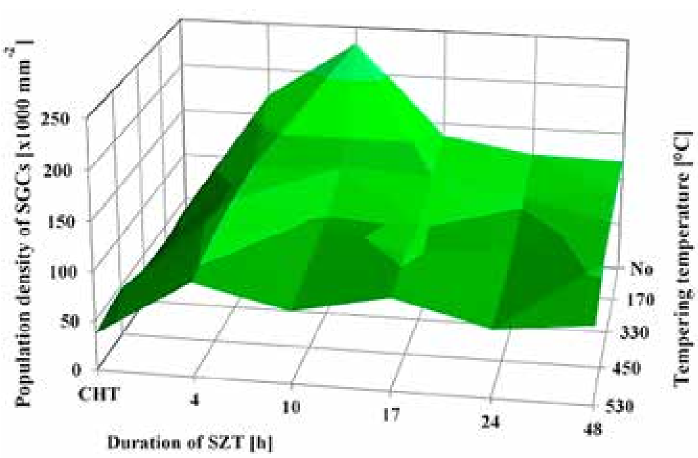

Figure 3: Population density of small globular carbides for differently sub-zero treated (at minus-75°C) and tempered specimens.

Tempering Temperature [°C]	No-Tempered	170	330	450	530
Retained austenite amount [vol%]	7.6±0.4	5.5±0.1	4.6±0.2	2.5±0.1	Not measurable

Table 3: Retained austenite amount (in vol%) in Vanadis 6 steel after quenching followed by sub-zero treatment at minus-75°C for 17 h, no-tempered and tempered at different temperatures.

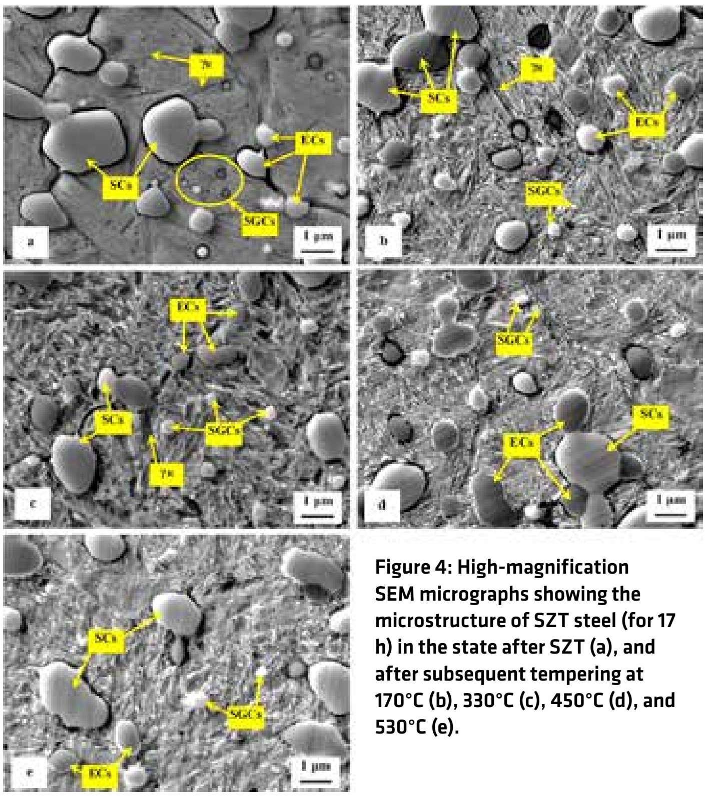

Figure 4: High-magnification SEM micrographs showing the microstructure of SZT steel (for 17 h) in the state after SZT (a), and after subsequent tempering at 170°C (b), 330°C (c), 450°C (d), and 530°C (e).

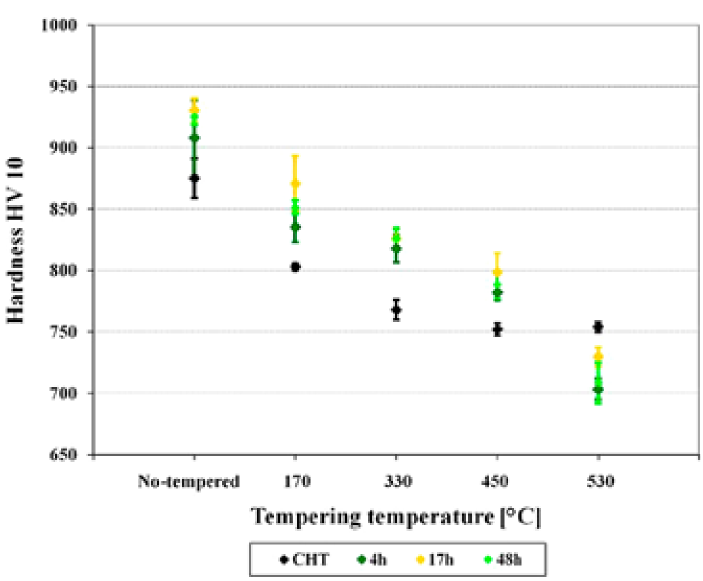

Figure 5: Hardness versus tempering temperature plots for conventionally heat-treated specimens and for specimens after sub-zero treatments at minus-75°C for different durations.

hardness values of the steel after sub-zero treatment at minus-75°C for 4, 17, and 48 hours were 908 ± 30, 930 ± 10, and 925 ± 6 HV10, respectively. Thus, the obtained results imply the hardness of the Vanadis 6 steel is higher due to the sub-zero treatments at minus-75°C, and that the hardness improvement reaches the maximum for the material treated for the duration of 17 hours. On the other hand, the hardness improvement is less significant than what was obtained by the treatment at lower SZT temperatures, e.g. at minus-140 or minus-196°C, where values exceeding 950 HV10 were obtained [12,22].

The hardness of conventionally quenched steel was 803, 768, 752, and 754 HV 10 after tempering at temperatures of 170, 330, 450, and 530°C, respectively. In other words, the hardness of conventionally heat-treated steel first decreases with increasing tempering temperature, and then it is preserved, almost constantly (at a level of 750 HV 10), when tempered at temperatures normally used for secondary hardening. In contrast, the steel after application of sub-zero treatments manifested higher hardness values, and this tendency was maintained up to the tempering temperature of 450°C. The most significant hardness improvement was recorded for the steel treated for 17 hours. For the specimens tempered at 530°C, however, the hardness of sub-zero treated steel was lower than what was obtained by CHT.

These results are in line with those obtained by investigations of tempering response of the steel after SZT at minus-196°C [12,20,21]. On the other hand, a strong variance between the tempering responses of the steel treated at minus-75°C and the steel treated at minus-140°C is evidenced. For the latter SZT temperature, it has been reported recently that hardness of the material was improved significantly within the whole range of tempering regimes used [22].

The flexural strength values obtained by three-point bend tests of samples having the microstructures according to Figure 4 are shown in Figure 6. It can be seen that the mean values of the flexural strength range between 3,300 and 3,700 MPa. The ranges of statistical uncertainty (at a probability level of 5 percent) overlap noticeably, suggesting the tempering has only a marginal effect on the flexural strength of SZT steel.

The work of fracture values of the steel tempered at 170, 330, and 450°C lie within the range of statistical uncertainty in Figure 6, suggesting low-temperature tempering does not influence this characteristic significantly. On the other hand, the work of fracture increases when the steel is tempered at temperature 530°C and above. This can be associated with hardness decrease (as indicated in Figure 6), and thus with more extensive (compared to what occur during testing of specimens tempered at lower temperatures) plastic deformation of the matrix.

It is also well visible that the W_{of} values follow closely the values of flexural strength, but only up to the tempering temperature of 530 C (peak of secondary hardness). For the specimens tempered at 600°C, however, this relationship is no more valid. At this place, it should be noted the Vanadis 6 steel belongs to the group of brittle steels when tempered at temperatures up to the secondary hardness peak; in these cases, the obtained values of flexural strength are an indirect measure of its toughness. On the other hand, the flexural strength loses the characteristic of toughness when the hardness of the steel decreases. This is the case of "overtempering" of the steel, i.e., when the steel is tempered at temperatures beyond the secondary hardness peak, for instance, at 600°C.

Figure 7 is a compilation of SEM micrographs showing fracture surfaces of flexural strength specimens that were sub-zero treated at minus-75°C for 17 hours and subsequently tempered at different temperatures. With respect to the surface morphology, the fracture surfaces can be divided into two groups. The fracture surfaces of the first group of specimens appear relatively flat with only very limited roughness caused by a strong difference between the fracture behavior of the matrix and carbides, Figure 7a-c. In contrast, the fracture surfaces (second group) of the specimens tempered at 530 and 600°C (the latter one in particular) manifest much more pronounced indications of plastic deformation of the matrix, Figure 7d,e. Here it should be noted the steel hardness decreased (and the plasticity expectedly increased) with increasing the tempering temperature in Figure 6. This correlates well with the earlier-mentioned morphology of fracture surfaces. In other words, the fracture surfaces appear relatively flat and shiny when the steel has higher hardness, but their topography increases with a hardness decrease (i.e., with increasing the tempering temperature).

Detailed SEM fractographs in Figure 8 clearly delineate the differences between the fracture surfaces obtained by testing of specimens tempered at 170 and 600°C. A relatively flat morphology of the fracture surface with only very limited plastic deformation of the matrix is visible in Figure 8a. The presence of micro-plastic deformation is only visible at the sites where decohesion at the matrix/carbide interface took place during the crack propagation. The sites with local micro-plastic deformation are mainly in close vicinity to smaller carbides, which act as decohesion sites at the earlier-mentioned interfaces. These carbides are denoted as decohesive carbides (DCs). Other carbide particles (the coarser ones in most cases) are cleaved, and they are denoted as "cleaved carbides, CCs." In contrast to the fracture surface shown in Figure 8a, the fracture of the specimen tempered at 600°C manifests much more pronounced plastic deformation shown in Figure 8b. However, the role of particular carbides in the crack propagation is maintained and is almost the same as shown in Figure 8a.

The obtained flexural strength values for differently sub-zero treated and tempered specimens are summarized in Figure 9. It is shown that the treatment at minus-75°C gave rather higher flexural strength than the conventional heat treatment. This is somewhat surprising at first glance, since one would expect a decrease in flexural strength rather than a slight increase due to the application of SZT.

To explain this, it should be noted that Vanadis 6 steel contains 20.2, 7.6, 4.8, 2.1, and 6.3 vol % of retained austenite after CHT, SZT at minus-75°C, SZT at minus-140°C, SZT at minus-196°C, and SZT at minus-269°C, respectively (all the SZTs were carried out for a 17-hour duration) [12,26]. Retained austenite is considered a soft microstructural feature, and one can expect its beneficial effect on toughness (and flexural strength). This may, for instance, partly explain the better flexural strength of the conventionally heat-treated material, as well as the material SZT at either minus-140 or minus-269°C, than was obtained by SZT at minus-196°C. However, this does not bring an answer to the improvement of flexural strength by SZT at minus-75°C, compared to CHT steel. As mentioned earlier, sub-zero treatment at minus-75 C produces a much higher population density of small globular carbides than CHT, which in turn leads to the formation of an increased number of matrix/carbide interfaces. The population density of small globular carbides decreases with tempering, despite remaining much higher than what can be obtained by CHT. In the steel samples with a higher population density of carbides, the crack propagation is probably more associated with micro-plastic deformation of a matrix (as Figure 8 clearly demonstrates); hence, an enhanced carbide count is an important factor responsible for improvements of flexural strength.

Finally, a few words should be written to the fact that the treatments at either minus-140 or minus-269°C lead to nearly equal or slightly better flexural strength than what is obtained in the present study. It has been reported recently that the treatment at minus-140°C for 17 hours results in the retained austenite amount of about

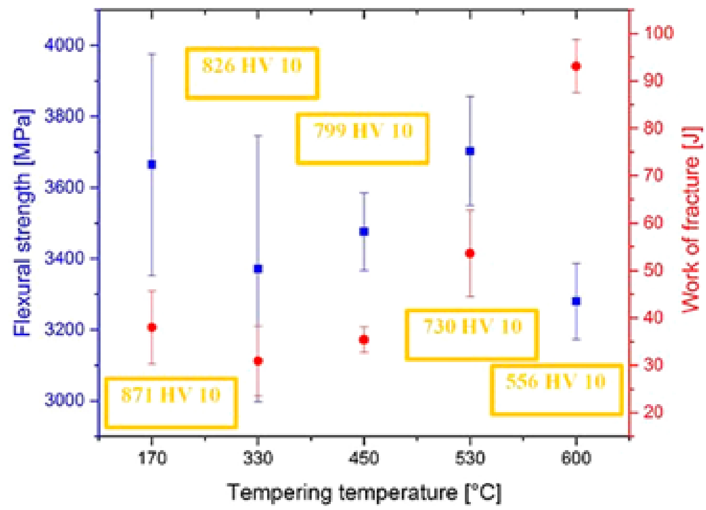

Figure 6: Flexural strength and work of fracture obtained by flexural three-point bend test for steel with application of SZT at minus-75°C for 17 h, and subsequent tempering.

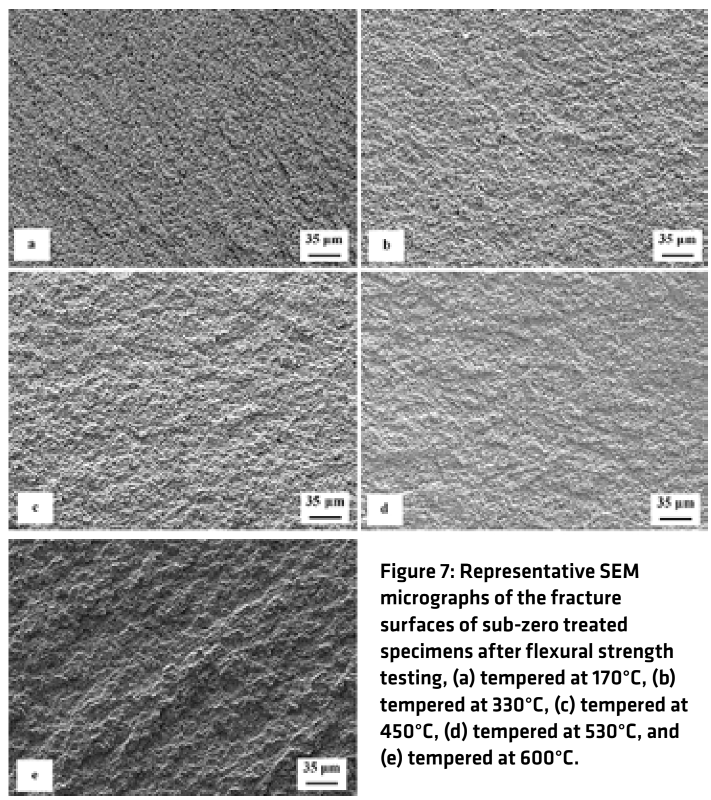

Figure 7: Representative SEM micrographs of the fracture surfaces of sub-zero treated specimens after flexural strength testing, (a) tempered at 170°C, (b) tempered at 330°C, (c) tempered at 450°C, (d) tempered at 530°C, and (e) tempered at 600°C.

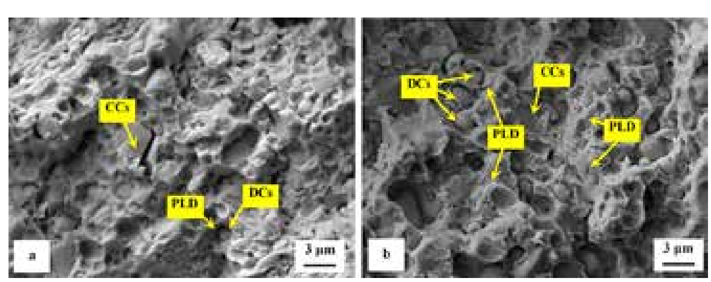

Figure 8: Detailed SEM micrographs of the fracture surfaces of sub-zero treated specimens after flexural strength testing, (a) tempered at 170°C and (b) tempered at 600°C.

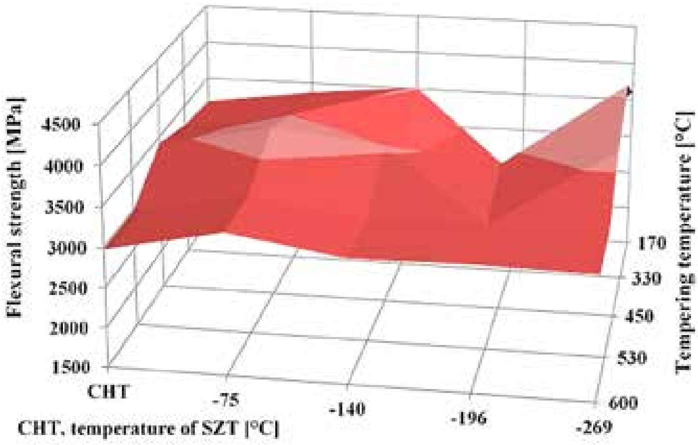

Figure 9: Comparison of the obtained flexural strength values for differently sub-zero treated and tempered specimens made of the Vanadis 6 steel.

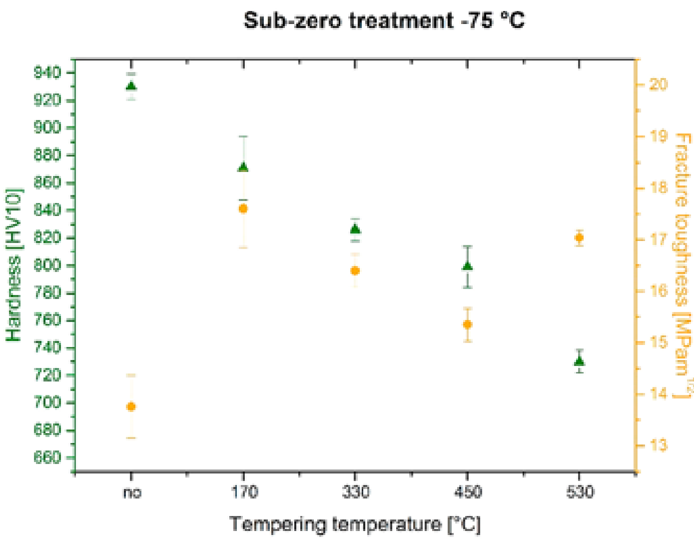

Figure 10: Fracture toughness versus hardness of the Vanadis 6 steel after SZT at minus-75°C for 17 h, and subsequent tempering.

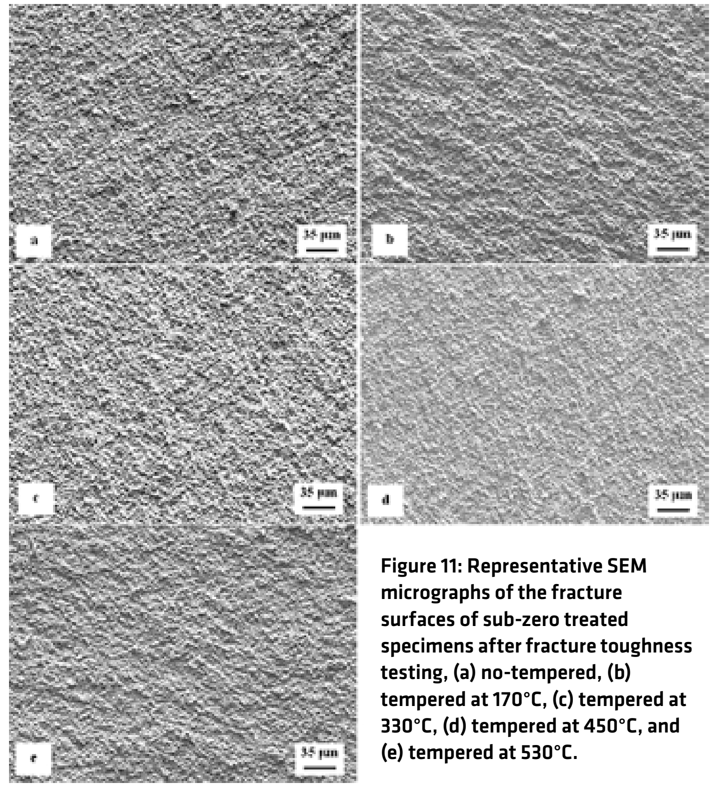

Figure 11: Representative SEM micrographs of the fracture surfaces of sub-zero treated specimens after fracture toughness testing, (a) no-tempered, (b) tempered at 170°C, (c) tempered at 330°C, (d) tempered at 450°C, and (e) tempered at 530°C.

4.3 vol% [22]. The latest measurements fixed the γ_R amount to 6.3 vol% in the Vanadis 6 steel treated in liquid helium. This is two times (for minus-140°C SZT) or three times (for minus-269°C) more than what was obtained by SZT at minus-196°C, but only of approximately 60% or 85% in comparison with the values reported here for SZT at minus-75°C. One can thus expect rather opposite tendency with respect to the changes of flexural strength; however, the treatment at minus-140°C (for instance) produces the greatest population density of SGCs, which more than fully compensates the toughness loss resulting from the reduction of retained austenite.

The relation between fracture toughness and hardness as a function of tempering temperature is seen in Figure 10. The fracture toughness values were 13.76 ± 0.61, 17.60 ± 0.75, 16.40 ± 0.32, 15.35 ± 0.32, and 17.04 ± 0.15 MPa × m$^{1/2}$ for specimens prior-to-tempering, tempered at 170, 330, 450, and 530°C, respectively. The lowest K_{IC} values were determined for prior-to-tempering specimens, which had the highest hardness. This is logical because the hardness is the key factor that influences the fracture toughness, and it is generally accepted that metals with high hardness usually manifest low fracture toughness level and vice versa [20,33]. However, the values of K_{IC} and hardness obtained by testing of tempered specimens do not obey this rule. It is, for instance, shown that the fracture toughness is high for the steel tempered at 170°C despite its high hardness. Further, the K_{IC} decreases along with the hardness when the tempering temperature is increased to either 330 or 450°C. An increase in K_{IC} was recorded only for the steel tempered at 530°C, but at a lower hardness value.

The analysis of fracture surfaces provides a more comprehensive insight into the variations of fracture toughness with tempering. Figure 11 is a compilation of representative SEM micrographs of the fractured K_{IC} specimens that were SZT at minus-75°C and no-tempered or tempered at different temperatures. The fracture surfaces of all the specimen-manifest symptoms that are typical for hard and brittle steels; they appear flat, shiny, and relatively smooth. However, more thorough investigation reveals differences on the topography of fractured surfaces. The surface of no-tempered specimen (Figure 11a) manifests much finer topography compared with the fractured surfaces of other specimens (Figure 11b-e). This can be attributed to the differences in fracture toughness-no-tempered specimens that have the lowest K_{IC} values, and tempering leads to moderate increase in this characteristic.

Detailed SEM micrographs in Figure 12 were acquired from the specimen that was not tempered after sub-zero treatment. The image in Figure 12a assists in seeing the fracture surface manifests typical morphology for hard steel. It contains a great number of micro-voids and holes, which correspond to the extraction of SGCs (in particular) from the fracture surface during the crack propagation. The formation of micro-voids is associated with local plastic deformation of the matrix. However, the capability of the matrix to be deformed plastically is very limited as seen in Figure 12b. There is a great number of sites with cleavage fracture mechanism apparent in the matrix as Figure 12c illustrates. The micrograph in Figure 12b also depicts the difference in behavior of carbides during the crack propagation. Some carbide particles (mainly the coarsest ones) were cleaved while others assisted the decohesion mechanism of the crack propagation. This is similar to what was discovered for the flexural strength specimens in Figure 8.

The role of particular carbides in the fracture propagation can be assessed with the help of recent investigations. It has been published recently that the coarsest particles belong mostly to the group of secondary carbides and that their nature is hexagonal M_7C_3 [7,11,12,22]. The finer particles are either eutectic carbides (MC-carbides with cubic crystallographic structure) or small globular carbides (cementite M_3C) [7]. Casellas et al. clearly demonstrated that lower symmetry of the hexagonal crystalline lattice (as compared with cubic MC phase) results in low fracture toughness of M_7C_3, and correspondingly in large scatter of its values (0.5-4.5 MPa × $m^{1/2}$) [34]. Moreover, Fukaura et al. [35] proved the size of the carbides plays an important role in their fracture propagation manner, namely that coarser particles are much more amenable to the cleavage than the finer carbides. In Vanadis 6 steel, the mean spherical diameter of the M_7C_3 particles is of around 2.5–2.8 μm while the MC carbides have size within the range 1.6–1.9 μm [26]. The size of small globular carbides, SGCs, is much smaller, below 0.5 μm. These facts assist to delineate the role of different carbides in fracture propagation as Figure 12 illustrates. Larger size and crystallographic anisotropy of M_7C_3 make this carbide more brittle than the MC (or M_3C), despite that the hardness of M_7C_3 is lower than that of MC [34]. This is why the most part of cleaved carbides are the SCs (M_7C_3) while a dominant number of ECs (and almost all the SGCs) is unaffected by the crack propagation, thus, assisting decohesion at the matrix/carbide interfaces.

The second series of detailed SEM micrographs, Figure 13, depicts the details of fracture propagation in the specimen that was sub-zero treated and subsequently tempered at 530°C. It is worth noting the fractured surfaces of specimens tempered at other temperatures did not differ significantly from that in Figure 13. Compared to the fracture surface of the prior-to-tempering specimen in Figure 12, the fracture surface of the tempered one contains much greater area fraction of micro-plastically deformed matrix seen in Figure 13a. Further, there are cleaved carbides (CCs) and decohesive carbides present.

The high-resolution SEM micrograph in Figure 13b shows details of cleaved secondary carbides (CCs) and decohesive eutectic carbide particles (ECs), suggesting the role of particular carbides in the fracture propagation is very similar to the case of the prior-to tempering specimen, see Figure 12. In other words, the difference in fracture toughness (13.76 ± 0.61 MPa × $m^{1/2}$ for the prior-to tempering steel versus 17.04 ± 0.15 MPa × $m^{1/2}$ for the steel tempered at 530°C) does not play a significant role in the fracture propagation mode of carbide particles. In contrast, mentioned difference in fracture toughness values is reflected in the matrix behavior. As Figure 13c illustrates, the fracture propagation on the matrix is associated with micro-plastic deformation, and the cleavage takes only a minor role. The differences in the fracture toughness, and correspondingly in the morphology of fracture surfaces of differently tempered specimens, can be explained considering the material microstructure. Table 3 shows the examined steel contains 7.6 ± 0.4 vol% of retained austenite in the prior-to-tempering state. The retained austenite is relatively soft, thus prone to plastic deformation. For instance, Putatunda [33] reported the retained austenite has a beneficial effect on the fracture toughness of high-carbon steels. However, the Vanadis 6 steel also contains a high amount of hard and brittle "pre-aged" martensite in the prior-to-tempering state. (It is worth noting aging of the martensite in sub-zero-treated high-carbon steels was many times experimentally proved, e.g. [14,15,26,36].) This makes the steel brittle. Berns and Broeckmann [1], Das et al. [19], and Ptačinová et al. [21] found the crack has a strong tendency to follow the interfaces between matrix and carbides when propagates during testing of ledeburitic steels. As a result, a micro-plastic deformation of the matrix occurs, which slightly improves the fracture toughness. Nevertheless, beneficial effects of retained austenite and increased population density of carbides cannot compensate the high brittleness of pre-aged martensite, hence, the material manifests very low fracture toughness as a consequence. Finally, it should be underlined that this finding is in line with the obtained results on the same steel but processed at different SZT temperatures as Figure 14 illustrates. Finally, it should be underlined that this finding is in line with the obtained results by the K_{IC} testing of the same steel that was processed at other SZT temperatures as Figure 14 illustrates.

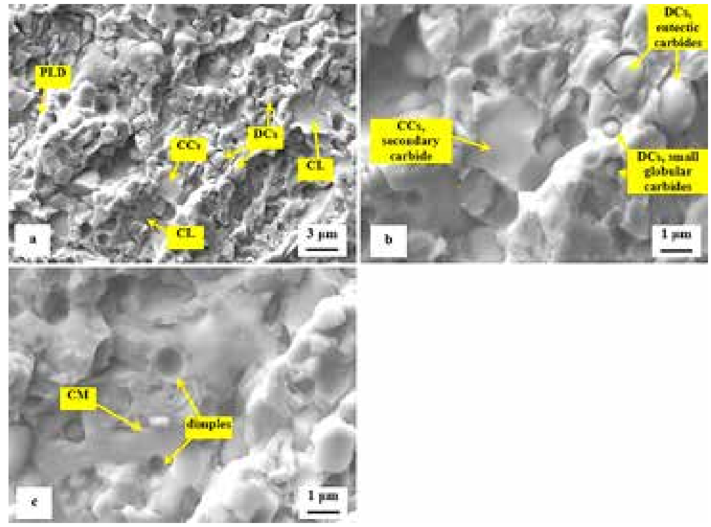

Figure 12: SEM images showing details of fracture propagation in sub-zero treated and no-tempered fracture toughness specimen, (a) detailed image showing the crack propagation in the matrix and the three main carbides including their role in fracture propagation, (CCs – cleaved carbides, DCs – decohesive carbides, PLD – plastic deformation in the matrix, CL – cleaved matrix), (b) high-magnification image showing cleaved M7C3 (CCs, secondary carbide), and decohesive particles that belong to eutectic carbides (DCs, eutectic carbides) and small globular carbides, and (c) high-magnification image showing cleaved matrix region (CM) and small dimples resulting from the extraction of small globular carbides.

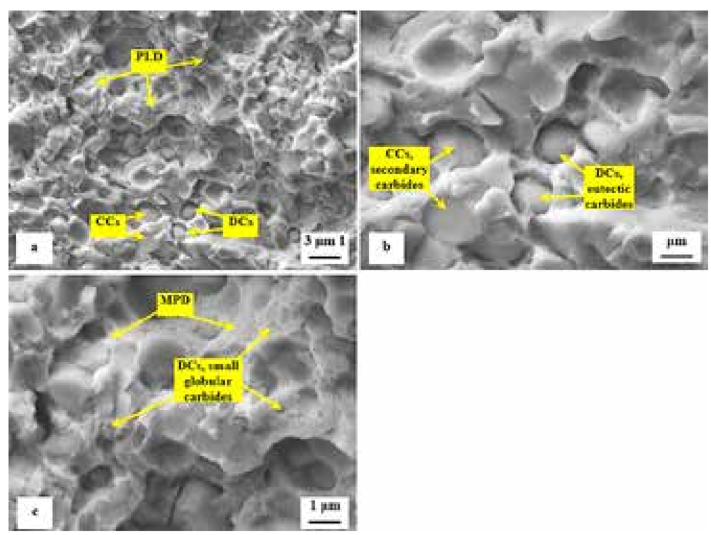

Figure 13: SEM images showing details of fracture propagation in sub-zero treated and subsequently tempered (at 530°C) fracture toughness specimen, (a) detailed image showing the crack propagation in the matrix and the three main carbides including their role in fracture propagation, (CCs – cleaved carbides, DCs – decohesive carbides, PLD – plastic deformation in the matrix), (b) high-magnification image showing cleaved M7C3 (CCs, secondary carbide), and decohesive particles that belong to eutectic carbides (DCs, eutectic carbides), and (c) high-magnification image showing micro-plastic deformation of the matrix (MPD) and small dimples resulting from the extraction of small globular carbides.

Tempering reduces the material hardness seen in Figure 5, and one

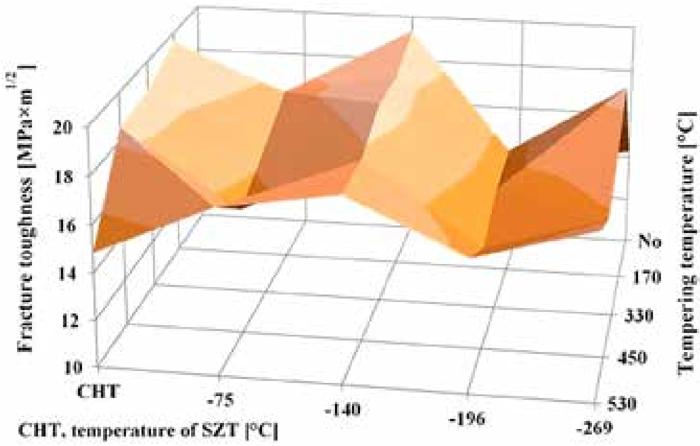

Figure 14: Comparison of the obtained fracture toughness values for differently sub-zero treated and tempered specimens made of the Vanadis 6 steel.

can thus expect an increase of fracture toughness. Increased fracture toughness was really recorded for sub-zero treated and subsequently tempered steel specimen seen in Figure 10. The clarification of this issue is relatively complex: On one hand, the amount of soft retained austenite is either moderately reduced (for the steel tempered at 170 or 330°C) or this phase is almost completely removed (after application of higher tempering temperatures), seen in Table 3. Also, tempering reduces the population density of small globular carbides, seen in Table 2 and in Figure 3. On the other hand, the martensite undergoes significant softening, which makes it more amenable to deform plastically. The resulting fracture toughness values are then a result of competition between the mentioned three phenomena. The increase of K_{IC} values can be mainly ascribed to the martensite softening, as this phase is the major one in the material. Increase in fracture toughness is reflected in more pronounced topography of fractured surfaces (and in more visible dimples on fracture surfaces at the same time). Compare Figure 11a with Figure 11b-e or Figure 12 with Figure 13.

A very interesting comparison of the current results with those obtained by testing of CHT steel and the steel that was subjected to SZT at minus-140, minus-196, or minus-269°C is provided in Figure 14. It is shown that the SZT at minus-140°C gave the best results that are fully comparable with conventionally heat-treated steel but at a significantly increased hardness as reported in [22]. Treatments at either the temperatures of boiling nitrogen or helium resulted rather in lower fracture toughness values.

A reliable explanation of the variations in fracture toughness is a very complex issue. In brief, the resulting fracture toughness value of ledeburitic tool steels is always a result of competition between three effects: 1) retained austenite amount, which undoubtedly acts in favor of higher K_{IC}, 2) state of the martensite (K_{IC} decrease), and 3) population density of small globular carbides (increase of K_{IC}) [22]. CHT steel contains about 20 vol% of the retained austenite in the prior-to-tempering state, and the retained austenite amount is nearly constant up to the tempering temperature of 500°C [12]. Even though the population density of SGCs is very low in CHT steel (as compared with the steel after SZTs), it is more than satisfactorily compensated by the retained austenite amount. Application of SZTs reduces the retained austenite amount considerably (with the minimum value for SZT at minus-196°C) and increases the population density of SGCs (with the maximum for the SZT at minus-140°C). The results in Figure 14 imply the reduction of retained austenite is almost fully compensated by a much higher population density of SGCs for the steel after SZT at minus-140°C, while other SZTs do not lead to a high enough population density of carbides needed to compensate the impact of reduced retained austenite amount on the resulting K_{IC} value.

Finally, it should be noted these considerations do not take into account the state of the martensite. In the state after CHT (and prior-to-tempering), the martensite was found to be "pre-aged," but it did not contain any carbide precipitates [7]. In contrast, the martensite after SZTs contained nano-sized, coherent transient carbides ([12,26]. However, it is hard or practically impossible to provide an exact assessment of the difference between impacts of these two martensite states on the fracture toughness of the steel since it also contains the retained austenite and several carbide types. The situation is very similar in the case of tempered steel Vanadis 6 because tempering leads to acceleration of precipitation rate at low-tempering temperatures but rather to delayed precipitation at high temperatures (around 500°C) [11,12,26]. But, an exact quantification of precipitates is almost impossible.

4 CONCLUSIONS

The impact of sub-zero treatment at the temperature of minus-75°C and subsequent tempering on the microstructure, hardness, flexural strength and fracture toughness was investigated. The main obtained results can be summarized as follows:

- The population density of small globular carbides is increased by the application of SZT at minus-75°C by the factor from the range 2.5 and seven.
- Retained austenite amount is reduced by this kind of treatment to an approximately one third as compared with conventional room temperature quenching.
- The bulk hardness of the steel is increased by SZT at minus-75°C, by 30-60 HV10. Improved steel hardness is maintained up to the tempering temperature of 450°C while tempering at 530°C leads to more significant hardness reduction than what is obtained by conventional heat treatment.
- The flexural strength of SZT steel ranges between 3,300 and 3,700 MPa. The level of tempering temperature has only a little impact in the flexural strength.
- The fracture toughness of sub-zero treated no-tempered steel is very low. However, it increases with the tempering application, and reaches relatively high values of around 17 MPa × $m^{1/2}$ after tempering to the secondary hardness peak.
- In summary, the application of SZT at minus-75°C may bring some benefits into heat treatment of tool steels. However, the obtained microstructures and values of mechanical properties are lower as compared, for instance, with those obtained by treatment at minus-140°C.

AUTHOR CONTRIBUTIONS

Funding acquisition, P.J.; Microstructural investigation, L.R.-T., P.J.; X-ray diffraction, M.K.; Dilatometry. J.K.; Flexural strength, fracture toughness testing, I.D.; Supervision, P.J.; Writing—original draft, review, editing, P.J., I.D.

FUNDING

The authors acknowledge that the paper is a result of experiments realized within the project VEGA 1/0264/17. In addition, this publication is the result of the project implementation "Centre for Development and Application of Advanced Diagnostic Methods in Processing of Metallic and Non-Metallic Materials – APRODIMET", ITMS: 26220120014, supported by the Research & Development Operational Programme funded by the ERDF.

CONFLICTS OF INTEREST

The authors declare no conflict of interest.

REFERENCES

[1] Berns, H.; Broeckmann, C. Fracture of Hot Formed Ledeburitic Chromium Steels. Eng. Fract. Mech. 1997, 58, 311-325.

[2] Das, D.; Ray, K.K. Structure-property correlation of cub-zero treated AISI D2 steel. Mater. Sci. Eng. A 2012, 541, 45-60.

[3] Amini, K.; Akhbarizadeh, A.; Javadpour, S. Investigating the effect of the quench environment on the final microstructure and wear behaviour of 1.2080 tool steel after deep cryogenic heat treatment. Mater. Des. 2013, 45, 316-322.

[4] Das, D.; Ray, K.K.; Dutta, A.K. Influence of temperature of sub-zero treatments on the wear behaviour of die steel. Wear 2009, 267, 1361-1370.

[5] Surberg, C.H.; Stratton, P.F.; Lingenhoele, K. The effect of some heat treatment parameters on the dimensional stability of AISI D2. Cryogenics 2008, 48, 42-47.

[6] Akhbarizadeh, A.; Javadpour, S.; Amini, K.; Yaghtin, A.H. Investigating the effect of ball milling during the deep cryogenic heat treatment of the 1.2080 tool steel. Vacuum 2013, 90, 70-74.

[7] Jurči, P.; Dománková, M.; Čaplovič, L.; Ptačinová, J.; Sobotová, J.; Salabová, P.; Prikner, P.; Šuštaršič, B.; Jenko, D. Microstructure and hardness of sub-zero treated and no tempered P/M Vanadis 6 ledeburitic tool steel. Vacuum 2015, 111, 92-101.

[8] Amini, K.; Akhbarizadeh, A.; Javadpour, S. Investigating the effect of holding duration on the microstructure of 1.2080 tool steel during the deep cryogenic treatment. Vacuum 2012, 86, 1534-1540.

[9] Tyshchenko, A.I.; Theisen, W.; Oppenkowski, A.; Siebert, S.; Razumov, O.N.; Skoblik, A.P.; Sirosh, V.A.; Petrov, J.N.; Gavriljuk, V.G. Low-temperature martensitic transformation and deep cryogenic treatment of a tool steel. Mater. Sci. Eng. A 2010, 527, 7027-7039.

[10] Villa, M.; Pantleon, K.; Somers, M.A.J. Evolution of compressive strains in retained austenite during sub-zero Celsius martensite formation and tempering. Acta Mater. 2014, 65, 383-392.

[11] Jurči, P. Sub-Zero Treatment of Cold Work Tool Steels–Metallurgical Background and the Effect on Microstructure and Properties. HTM J. Heat Treat. Mater. 2017, 72, 62-68.

[12] Jurči, P.; Dománková, M.; Hudáková, M.; Ptačinová, J.; Pašák, M.; Palček, P. Characterization of microstructure and tempering response of conventionally quenched, short- and long-time sub-zero treated PM Vanadis 6 ledeburitic tool steel. Mater. Charact. 2017, 134, 398-415.

[13] Stratton, P.F. Optimizing nano-carbide precipitation in tool steels. Mater. Sci. Eng. A 2007, 449-451, 809-812.

[14] Van Genderen, M.J.; Boettger, A.; Cernik, R.J.; Mittemeijer, E.J. Early Stages of Decomposition in Iron-Carbon and Iron-Nitrogen Martensites: Diffraction Analysis Using Synchrotron Radiation. Metall. Trans. A 1993, 24, 1965-1973.

[15] Preciado, M.; Pellizzari, M. Influence of deep cryogenic treatment on the thermal decomposition of Fe-C martensite. J. Mater. Sci. 2014, 49, 8183-8191.

[16] Collins, D.N.; Dormer, J. Deep Cryogenic Treatment of a D2 Cold-work Tool Steel. Heat Treat. Met. 1997, 3, 71-74.

[17] Wierszyllowski, I. The Influence of Post-quenching Deep Cryogenic Treatment on Tempering Processes and Properties of D2 Tool Steel. Studies of Structure, XRD, Dilatometry, Hardness and Fracture Toughness. Defect Diffus. Forum 2006, 258-260, 415-420.

[18] Rhyim, Y.M.; Han, S.H.; Na, Y.S.; Lee, J.H. Effect of Deep Cryogenic Treatment on Carbide Precipitation and Mechanical Properties of Tool Steel. Solid State Phenom. 2006, 118, 9-14.

[19] Das, D.; Sarkar, R.; Dutta, A.K.; Ray, K.K. Influence of sub-zero treatments on fracture toughness of AISI D2 steel. Mater. Sci. Eng. A 2010, 528, 589-603.

[20] Sobotová, J.; Jurči, P.; Dlouhý, I. The effect of sub-zero treatment on microstructure, fracture toughness, and wear resistance of Vanadis 6 tool steel. Mater. Sci. Eng. A 2016, 652, 192-204.

[21] Ptačinová, J.; Sedlická, V.; Hudáková, M.; Dlouhý, I.; Jurči, P. Microstructure Toughness relationships in sub-zero treated and tempered Vanadis 6 steel compared to conventional treatmen. Mater. Sci. Eng. A 2017, 702, 241-258.

[22] Jurči, P.; D˘ urica, J.; Dlouhý, I.; Horník, J.; Planieta, R.; Kralovič, D. Application of -140°C Sub-Zero Treatment For Cr-V Ledeburitic Steel Service Performance Improvement. Metall. Mater. Trans. A 2019, 50, 2413-2434.

[23] Kumar, S.; Nahraj, M.; Bongale, A.; Khedkar, N.K. Effect of deep cryogenic treatment on the mechanical properties of AISI D3 tool steel. Int. J. Mater. Eng. Innov. 2019, 10, 98-113.

[24] Reitz, W.; Pendray, J. Cryoprocessing of Materials: A Review of Current Status. Mater. Manuf. Process. 2001, 16, 829-840.

[25] Gavriljuk, V.G.; Theisen, W.; Sirosh, V.V.; Polshin, E.V.; Kortmann, A.; Mogilny, G.S.; Petrov, Y.N.; Tarusin, Y.V. Low-temperature martensitic transformation in tool steels in relation to their deep cryogenic treatment. Acta Mater. 2013, 61, 1705-1715.

[26] Ďurica, J.; Ptačinová, J.; Dománková, M.; Čaplovič, L.; Čaplovičová, M.; Hrušovská, L.; Malovcová, V.; Jurči, P. Changes in microstructure of ledeburitic tool steel due to vacuum austenitizing and quenching, sub-zero treatments at minus-140°C and tempering, Vacuum 2019. 2019.

[27] Zurecki, Z. Cryogenic Quenching of Steel Revisited. In Proceedings of the 23rd Heat Treating Society Conference, Pittsburgh, PA, USA, 26–28 September 2005; pp. 106-114.

[28] ASTM E975-13. Standard Practice for X-Ray Determination of Retained Austenite in Steel with Near Random Crystallographic Orientation; ASTM Book of Standards: West Conshohocken, PA, USA, 2004; Volume 3.01.

[29] CSN EN ISO 6507-1. Metallic Materials - Vickers Hardness Test - Part 1: Test Method; Office for Technical Standardization, Metrology and State Testing: Prague, Czech Republic, 2018.

[30] Jurči, P.; Dlouhý, I. Fracture Behaviour of P/M Cr-V Ledeburitic Steel with Different Surface Roughness. Mater. Eng. 2011, 18, 36-43.

[31] CSN EN ISO. Hardmetals – Determination of Transverse Rupture Strength; Office for Technical Standardization, Metrology and State Testing: Prague, Czech Republic, 2009.

[32] ISO 12135. Metallic Materials – Determination of Plane Strain Fracture Toughness. 2010. Available online: https://www.iso.org/standard/60891.html (accessed on 1 November 2016).

[33] Putatunda, S.K. Fracture toughness of a high carbon and high silicon steel. Mater. Sci. Eng. A 2001, 297, 31-43.

[34] Casellas, D.; Caro, J.; Molas, S.; Prado, J.M.; Valls, I. Fracture toughness of carbides in tool steels evaluated by nanoindentation. Acta Mater. 2007, 55, 4277-4286.

[35] Fukaura, K.; Yokoyama, Y.; Yokoi, D.; Tsuji, N.; Ono, K. Fatigue of cold-work tool steels: Effect of heat treatment and carbide morphology on fatigue crack formation, life, and fracture surface observations. Metall. Mater. Trans. A 2004, 35, 1289-1300.

[36] Cheng, L.; Brakman, C.M.; Korevaar, B.M.; Mittemeijer, E.J. The tempering of iron-carbon martensite; dilatometric and calorimetric analysis. Metall. Trans. A 1988, 19, 2415-2426.

ABOUT THE AUTHORS

Martin Kusý, Lýdia Rízeková-Trnková, Jozef Krajčovič, and and Peter Jurči are with the Institute of Materials Science, Faculty of Materials Science and Technology in Trnava, Paulínská 16, 917 24 Trnava, Slovakia; martin.kusy@stuba.sk (M.K.); lydia.trnkova@stuba.sk (L.R.-T.); jozef_krajcovic@stuba.sk (J.K.) Ivo Dlouhý is with the Institute of Physics of Materials, CEITEC-IPM, Czech Academy of Sciences, Zizkova 22, 61662 Brno, Czech Republic; idlouhy@ipm.cz

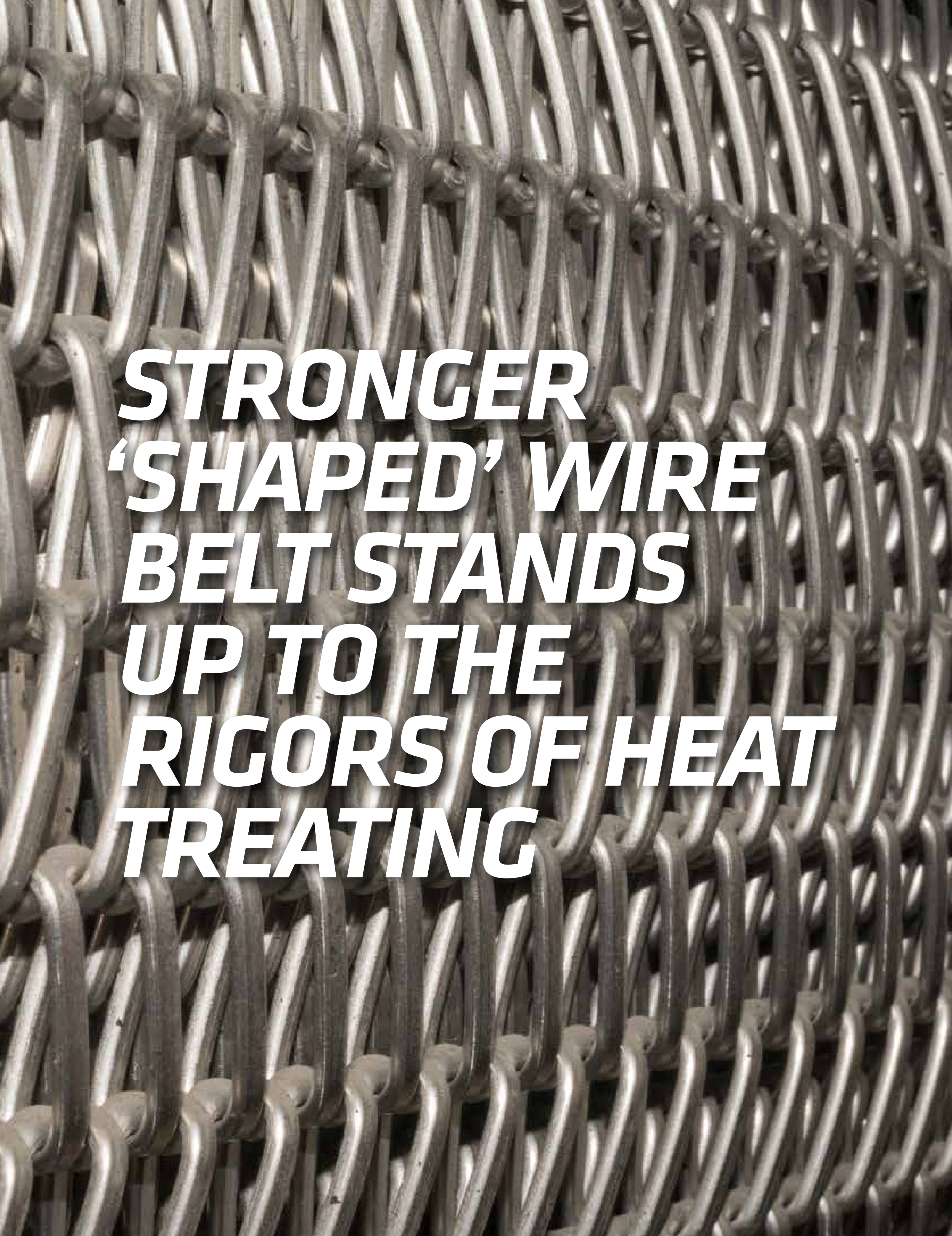

STRONGER 'SHAPED' WIRE BELT STANDS UP TO THE RIGORS OF HEAT TREATING

Engineered geometry increases strength, decreases stretch, and withstands thermal cycling.

By DEL WILLIAMS

Whether for automotive, aerospace, or heavy equipment, manufacturers using heat treatment — which can reach temperatures up to 2,400°F and vary from a few seconds to 60-plus hours — need conveyor belting that can withstand the rigors of the process. However, traditional round balance weave wire belting has changed little in 100 years and often requires annual replacement, causing costly production downtime.

Heat treating is essential to improve the properties, performance, and durability of metals such as steel, iron, aluminum alloys, copper, nickel, magnesium, and titanium. This can involve conveying to hardening, brazing, and soldering, as well as to sintering furnaces, carburizing furnaces, atmosphere tempering furnaces, and heat processing in annealing and quenching furnaces. Parts treated can range from bearings, gears, axles, fasteners, camshafts, and crankshafts to saws, axes, and cutting tools.

PROLONGING BELT LIFE

Heat treat-grade balance weave belts — made of temperature-resistant stainless steel or other heat-resistant alloys suitable to be run on a conveyor with friction drive — can cost thousands of dollars, depending on the dimensions and quality. So, even though wear and premature replacement seems inevitable, such wire belting should not be considered a low-cost consumable. While many manufacturers using heat treating consider periodic replacement of wire belting simply a cost of doing business, today, innovative alternatives have been developed that can significantly prolong its life and drive down operational cost.

Although heat-resistant wire belting is available, repeated thermal cycling between heating, soaking, and cooling while carrying substantial loads can continually weaken its structure until it fails. The greater and more frequent the temperature fluctuations in heat treatment steps, the shorter the wire belt's usable life becomes.

In addition, on conveyor belts, belt stretch accelerated by heat and dynamic loading forces on the belt is typically the main cause of breakage and failure.

Fortunately, industry innovation in the form of engineered, "shaped" wire belting has minimized these challenges. The design vastly prolongs usable life with increased strength and decreased stretch, which dramatically curtails replacement costs and production downtime.

This approach can also help to extend the longevity of wire belting used with increasingly popular powder metal parts, particularly sintered parts that may be heat treated to enhance strength, hardness, and other properties. In such cases, powder metal serves as a feed stock that can be processed into a net-shape without machining.

RESOLVING THE CORE ISSUES

Although conventional round wire belt has been the industry standard for generations, the geometry of the wire itself contributes to the problem.

Traditional round wire belt and even top-flattened wire belting is prone to belt stretch and premature replacement, particularly under high heat treatment temperatures. In testing, typical round and top flattened conveyor wire belt have been observed to stretch approximately 7 percent.

Even though many producers of conveyor wire belting simply import semi-finished product and finish it domestically, at least one U.S.-based manufacturer has gone to the root of the problem.

"Shaped" wire is designed to provide more strength in wire belt of a given diameter that can better withstand high heat processing

Heat treat-grade balance weave belts can cost thousands of dollars, depending on the dimensions and quality. (Courtesy: Lumsden)

The innovative design is significantly extending the usable life of wire-belt conveyors used in a variety of heat-treat processes. This ranges from hardening, brazing, and soldering to sintering, carburizing, and atmosphere tempering furnaces.

Many manufacturers using heat treating consider periodic replacement of wire belting simply a cost of doing business. (Courtesy: Lumsden)

conditions. This significantly prolongs its usable life up to eight times or more.

As an example, one engineered wire belt, called Sidewinder by Lancaster, Pennsylvania-based Lumsden Belting, a manufacturer of metal conveyor belts for industrial heat treatment, compresses and expands wire so it is taller than it is wide with flat sides.

To begin with, the patented side flattened wire's "I-beam" design provides three times greater structural support for heat-treated parts compared to standard round wire. The added height of the wire also provides a longer wear life without needing heavier wire. Together, the design limits belt stretch to only 1 to 2 percent. This minimizes the potential for damaged belt. Minimal belt stretch also helps the conveyor belt to track straighter, improving production throughput with less required maintenance.

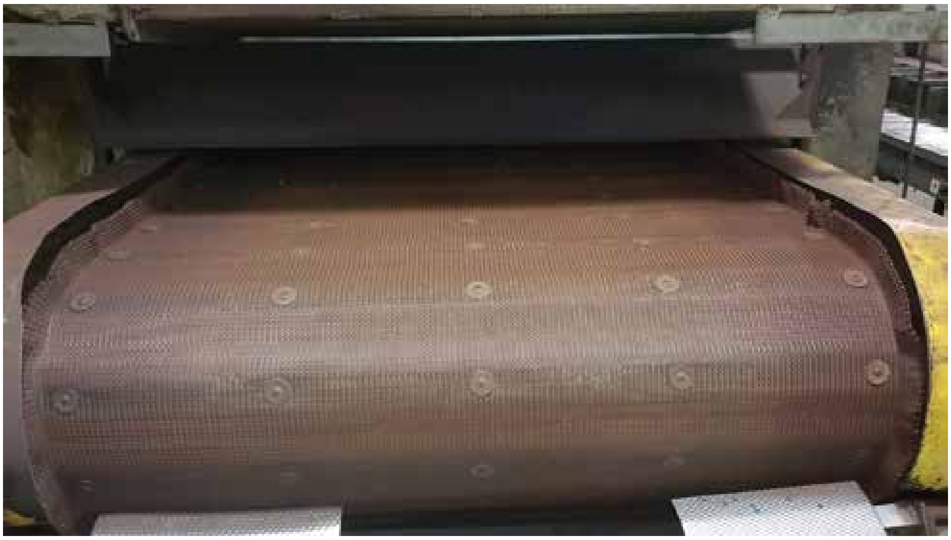

Wire belting should not be considered a low-cost consumable. (Courtesy: Lumsden)

INNOVATIVE DESIGN

The innovative design is significantly extending the usable life of wire-belt conveyors used in a variety of heat-treat processes. This ranges from hardening, brazing, and soldering to sintering, carburizing, and atmosphere tempering furnaces.

It is also prolonging wire-belt conveyor life in secondary powder-metal processes used to improve hardness and other mechanical properties. In this vein, it could be used in a mesh belt sintering furnace, where compacted parts are placed in a controlled atmosphere and heated. It could also be used in processes such as quench and temper, case carburizing, and induction hardening.

When heat treatment is used for hardening, followed by rapid cooling submerged in a medium such as oil, brine, or water, the shaped wire belt also enhances the open area for the same gauge wire. This reduces residue build up and eases cleaning while minimizing drag.

Although the cost of the shaped wire belt is slightly more than traditional round wire, for manufacturers relying on heat treatment, the gains in lifespan and production uptime can provide a speedy ROI.

ABOUT THE AUTHOR

Del Williams is a technical writer based in Torrance, California. For more information, go to www.lumsdencorp.com.

CUSTOMIZATION, TECHNOLOGY, AND QUALITY

A cart bottom furnace, model H15. It is used for component brazing in the aviation sector. (Courtesy: TAV VACUUM FURNACES)

TAV VACUUM FURNACES designs and manufactures top-quality vacuum furnaces for a wide range of industries and applications worldwide.

By KENNETH CARTER, Thermal Processing editor

TAV VACUUM FURNACES is an Italian company founded in 1984 by Giuseppi Tonini and a group of entrepreneurs active in the field of heat treatment. The strong entrepreneurial spirit, engineering skills, and hard work has led TAV VACUUM FURNACES to be one of the players in the production of high-quality vacuum furnaces.

"Our company has an established presence in the European market and, in the past decades, we were grown our presence in Chinese, North American, and Asia Pacific market," said Guido Locatelli, general manager of TAV VACUUM FURNACES. "Throughout the years, we have developed a deep understanding of customer's needs and how to best cater to them with quality service."

TAV's vacuum furnaces are used in a wide range of heat treatments for different materials such as steels, alloys, superalloys, advanced ceramic, for hardening, solubilization, annealing, brazing, and sintering. They are mainly applied in the following sectors: production of heat exchangers, aviation/aerospace, automotive, IGT (industrial gas turbine), additive manufacturing, commercial heat treatment, and the component sintering industry (medical, precision mechanics, optics, fashion).

"Flexibility, technology, and quality are the core values of our company," Locatelli said.

FLEXIBILITY

The company's customers recognize TAV VACUUM FURNACES as a proven and reliable solution provider in vacuum technology, according to Locatelli.

"Our extensive vacuum furnace line is proof of our flexibility," he said.

TAV VACUUM FURNACES designs and manufactures vacuum furnaces with different configurations, range of temperatures, and working pressure. Horizontal vacuum furnaces with a hinged door, horizontal vacuum furnaces with a cart bottom door, and vertical vacuum furnaces with a top or bottom load are all part of of TAV's portfolio.

The company's furnaces can work in a wide range of temperatures up to 2,800°C, and with pressure from the Ultra High Vacuum, it can be used in nuclear and research laboratories up to 150 bars for hot isostatic pressure applications.

"All our products could be highly customized in order to meet customer needs and achieve the best integration in their production plants and processes," Locatelli said.

TECHNOLOGY

Through its large team of experienced mechanical and automation engineers and supported by the most advanced software and instrumentation, TAV VACUUM FURNACES provides timely and qualified solutions to its customers, according to Locatelli.

"TAV VACUUM FURNACES has heavily invested in our R&D department in the last two years," he said. "Through collaboration with universities and research centers, our R&D department is implementing and validating new processes and technologies that will be implemented in our products."

The department is focused on following and supporting its customers from the beginning, according to Locatelli. Customers can benefit from a close and strong collaboration. Heat treatment, for sample, metallurgical analyses, and hardness tests can be performed in TAV's R&D department to help customers proof, fine-tune, and validate their processes.

A vapor-phase aluminizing furnace, model TPA 72-78. (Courtesy: TAV VACUUM FURNACES)

QUALITY

"TAV is strongly committed to quality in his widest meaning," Locatelli said. "A big effort was spent in the past years in developing a very strong quality department."

TAV's quality department supervises all activities from the acquisition of materials to the fine-tuning of its products with a view to a global quality concept.

"All our furnaces are fully tested in our company by quality team engineers before they're accepted and delivered to our customers," Locatelli said. "The quality department supervises all commissioning and testing at the customer's premises in order to guarantee the best

A semi-continuous furnace, model TBHA 45-180-365. It is used for aluminum brazing of components in the aviation sector. (Courtesy: TAV VACUUM FURNACES)

results and performances."

TAV's structure is so strongly committed to quality that the service department is under the umbrella of quality, too, according to Locatelli. Service and after sales job are performed through a network of companies: FURNACARE Inc. for the North American market and TAVENGINEERING for the rest of the world.

"Service and manufacturing require different attitudes," Locatelli said. "Service jobs must be fast and effective while manufacturing requires stringent planning and a deep understanding of the problems."

The laboratory at TAV VACUUM FURNACES' R&D department. (Courtesy: TAV VACUUM FURNACES)

LOOKING TO THE FUTURE

As the heat-treat industry has evolved, TAV VACUUM FURNACES has continued to evolve with it.

The continued growth of the industry has TAV looking to the future at how established technology can be used with new innovations already making waves. One of those, according to Locatelli, is additive manufacturing.

"There are some new processes that are coming with additive manufacturing, like binder jetting, that will for sure grow the market in the future," he said. "There will be a lot of requests and demand for furnaces for that kind of process. Most of the parts obtain with AM process needs to be heat treated, especially with binder jetting. This technology will move the AM parts to large volume production, whereas laser sintering now is focused on smaller volumes."

Locatelli said TAV plans to keep a sharp eye on the future as it looks to keep growing.

A vacuum furnace is the safer and more environmentally friendly heat-treatment process, and Locatelli expects this market will continue to grow.

"The increased attention to environmental and safety issues will lead to a greater demand for vacuum furnaces in the future," he said. "Producers of vacuum furnaces are constantly looking for better performance of their products in order to replace the use of traditional heat treatments such as quenching in oil or salt baths."

Using environmentally sustainable equipment is an important mission for TAV in that many industries, including automotive, are looking to manufacture parts without any potentially hazardous implications, according to Locatelli.

"The vacuum heat-treatment process is surely a sustainable technology," he said. "And TAV is working to develop high-performance furnaces to replace traditional heat treatment."

MORE INFO www.tav-vacuumfurnaces.com

A vertical bottom load furnace, model TPVH - SE 230-300 all metal. It is used to treat turbines blades in the aviation sector. (Courtesy: TAV VACUUM FURNACES)

MARKETPLACE ///

Manufacturing excellence through quality, integration, materials, maintenance, education, and speed.

Contact **Thermal Processing** at 800-366-2185 to feature your business in the Marketplace.

ADVERTISER INDEX ///

Q&A /// INTERVIEW WITH AN INDUSTRY INSIDER

STEPHEN HARRIS /// CHIEF EXECUTIVE /// BODYCOTE GROUP

"Bodycote Elgin will better serve the Midwest region with improved customer service and additional technology offerings such as nitriding, Corr-I-Dur, nitrocarburizing and low-pressure carburizing (LPC) solutions."

Tell us about the new Bodycote Elgin, Illinois, facility. When did it become fully operational?

We are very pleased to announce that our brand-new Elgin facility, Illinois, located northwest of Chicago, is now fully operational and supporting customer requirements. We started the upgrade and installation of the new facility in early 2020 with the vision to create a state-of-the-art facility to serve the Upper Midwest region. The site opened in early December 2020.

What was the reason for building the new upgraded facility?

The facility is designed as a replacement for an aging facility in Melrose Park, Illinois. As we evolve and incorporate the latest technologies into our processes, we also consider each of our facilities capabilities to deliver maximum value for our customers. We announced earlier last year that we would replace the Melrose Park facility and invest in a plant that will provide all of the benefits of a fully engineered and coordinated model for safety, quality, and cost.

We are committed to ensuring we are able to meet our customers' demands in the years ahead. The location reflects Bodycote's commitment to serving the Midwest manufacturing supply chains and allows us to shape the future of both our company and the industries we serve.

Bodycote's Elgin facility, Illinois, located northwest of Chicago, is fully operational and supporting customer requirements. (Courtesy: Bodycote)

What types of services are available at the facility?

Bodycote continues to provide gas-carburizing, stress-relieving, and vacuum hardening as previously offered at the Melrose Park location. The new facility also provides additional solutions including nitriding, Corr-I-Dur, nitro-carburizing, and low-pressure carburizing (LPC). As the Elgin facility is designed specifically to our specification, we can limit process variation and provide cost advantages to our customers.

What kind of customer requirements has the facility accounted for?

Bodycote upgraded our capabilities with the Elgin operations to ensure delivery of the best possible efficiency and geographical network to serve customers from the agricultural, mining, construction, automotive, and various other manufacturing supply chains in the region. A key driver to expanding our customer partnerships includes supporting growth into new technologies, using more efficient equipment, and supporting developing markets. This Elgin facility is capable of gaining certification for a full spectrum of market-support requirements, including aerospace and more.

How will this facility better serve the Midwest?

Bodycote Elgin will better serve the Midwest region with improved customer service and additional technology offerings such as nitriding, Corr-I-Dur, nitrocarburizing and low-pressure carburizing (LPC) solutions. We look forward to continuing our investment in this facility to ensure that customers experience a local service with superior quality and turnaround time.

The new location allows for increased thermal processing capabilities and will enable us to match our technology strengths with the market requirements in the Midwest. The growing demand for reliable precision components aligns with our service offerings at this new facility allowing Bodycote to create value for our customers and meet their demands.

We look forward to hosting an official opening event when COVID-19 related restrictions are lifted.

MORE INFO www.bodycote.com


YOU'VE GOT THE PRODUCTS.
YOU'VE GOT THE SERVICES.
NOW, LET US SHARE YOUR STORY.
Thermal Processing wants to make sure the best possible audience knows your company. Through our print, online, and social media presence, our experienced staff can get your message to an industry that wants to know what you can do.
Thermal processing
To learn more, contact national sales director Dave Gomez at dave@thermalprocessing.com or call 800.366.2185 ext. 207


HIGH TEMPERATURE HEAT
TREATMENT IS OUR SPECIALTY.
Across International equipment features targeted and precise temperature control, high quality components, and sophisticated features, all at a great price.
ACROSS INTERNATIONAL
Material Processing Equipment
AcrossInternational.com
For all your heat treatment needs, choose Across Internaional.
888-988-0899 Ext 2
@acrossinternational